united nations
educational, scientific
and cultural
organization

international atomic
energy agency

the
abdus salam
international centre for theoretical physics

H4. SMR/1247
Lecture Note: 08

WORKSHOP ON PHYSICS OF MESOSPHERE-STRATOSPHERE-TROPOSPHERE INTERACTIONS WITH SPECIAL EMPHASIS ON MST RADAR TECHNIQUES

(13 - 24 November 2000)

AN INTRODUCTION TO RADAR TECHNIQUES FOR STUDIES OF THE IONOSPHERE, MESOSPHERE, STRATOSPHERE AND TROPOSPHERE

Prof. Jurgen ROTTGER

Max-Planck-Institut fur Aeronomie
Katlenburg-Lindau
GERMANY

Second International School
of Atmospheric Radar - ISAR2
Hilton Head Island, SC, USA
5-6 November 1995

An Introduction to Radar Techniques for Studies of the Ionosphere, Mesosphere, Stratosphere and Troposphere

Jürgen Röttger
EISCAT Scientific Association
P.O. Box 812
S-981 28 Kiruna, Sweden

(A)

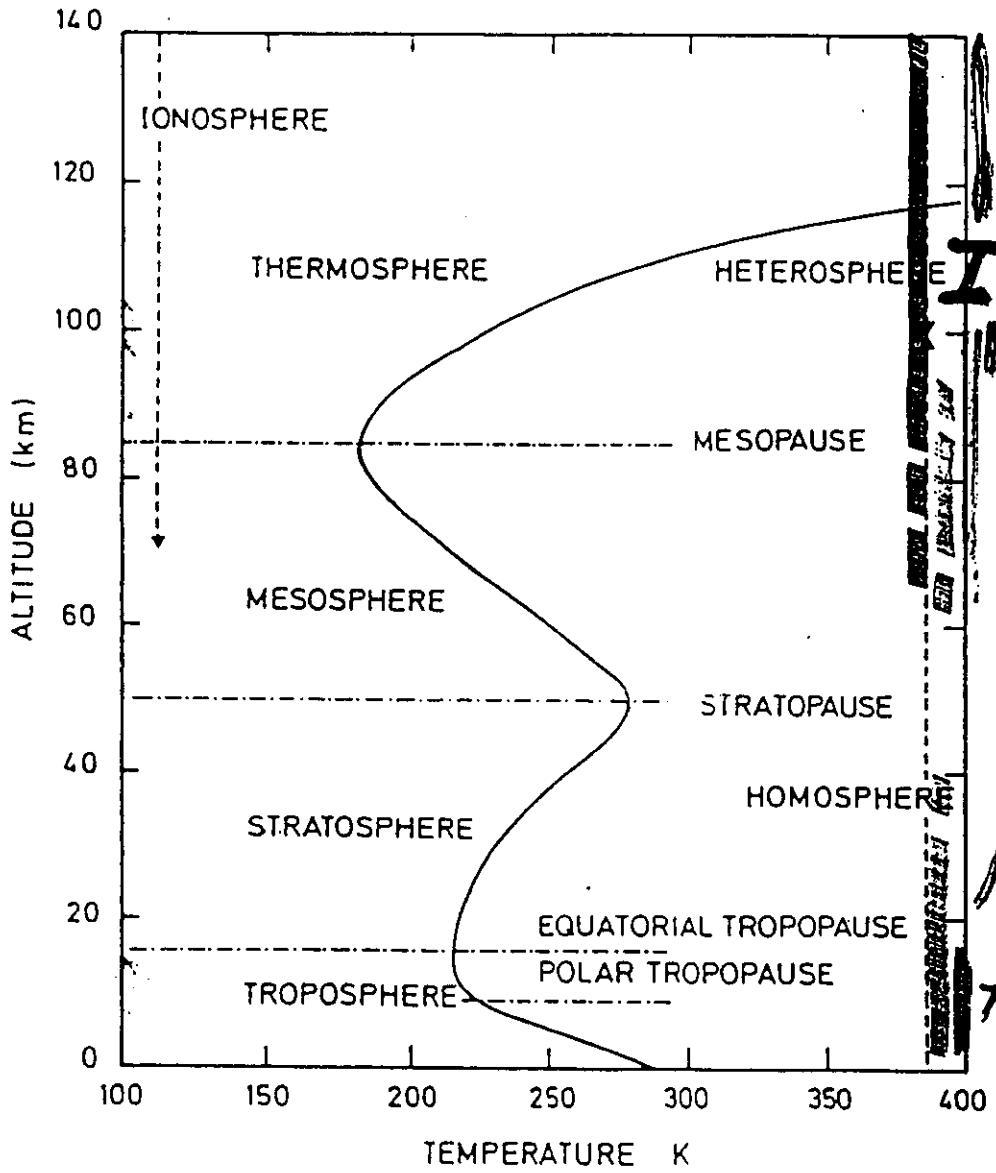
140
120
100
80
60
40
20
0
ALTITUDE (km)
IONOSPHERE
THERMOSPHERE
HETEROSPHERE
MESOPAUSE
MESOSPHERE
STRATOPAUSE
HOMOSPHERE
STRATOSPHERE
EQUATORIAL TROPOPAUSE
POLAR TROPOPAUSE
TROPOSPHERE
100
150
200
250
300
350
400
TEMPERATURE K

A01

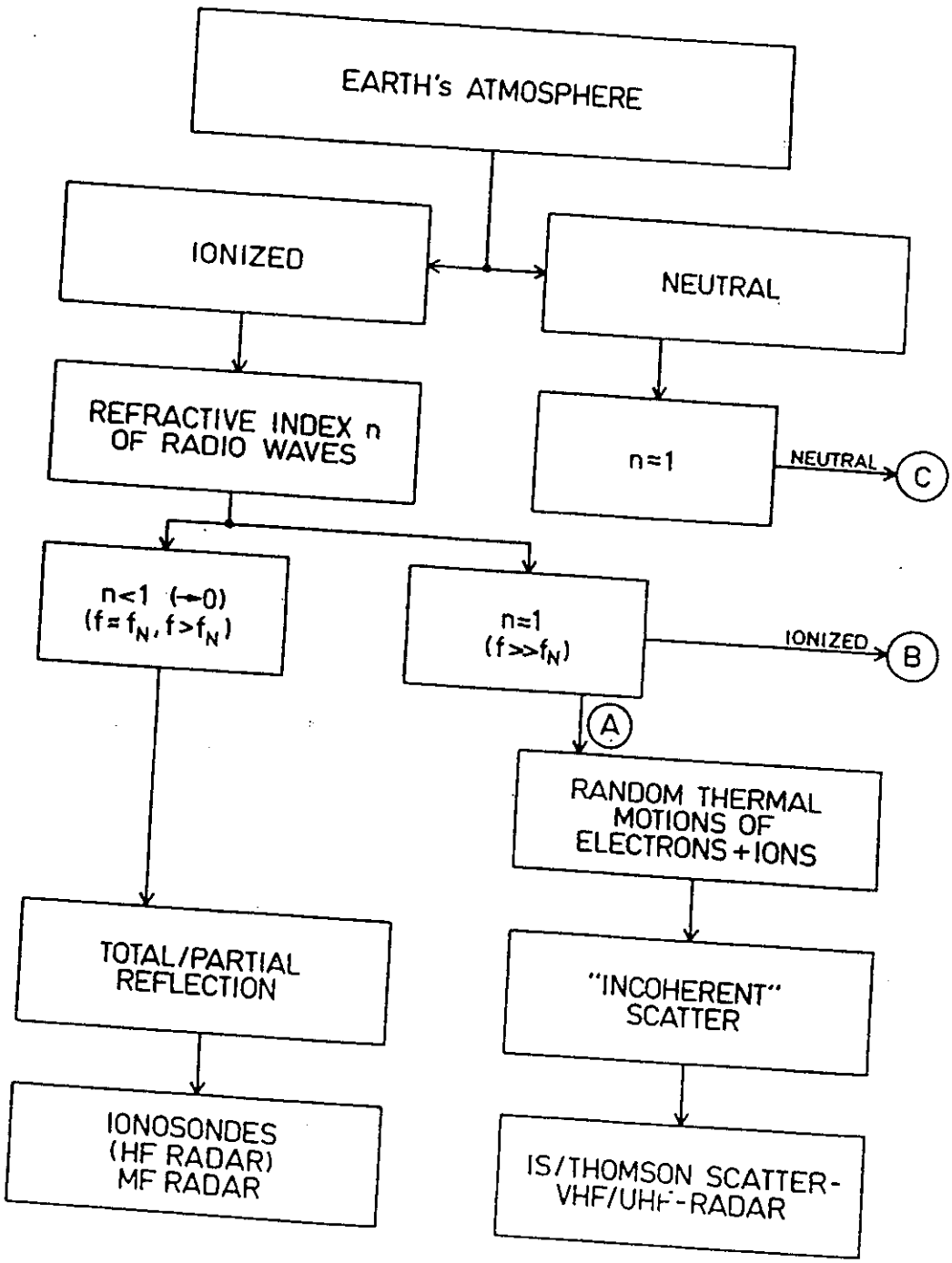
EARTH's ATMOSPHERE
IONIZED
NEUTRAL
REFRACTIVE INDEX n OF RADIO WAVES
n≈1
NEUTRAL
C
n<1 (→0) (f≈f_N, f>f_N)
n≈1 (f>>f_N)
IONIZED
B
A
RANDOM THERMAL MOTIONS OF ELECTRONS + IONS
TOTAL/PARTIAL REFLECTION
"INCOHERENT" SCATTER
IONOSONDES (HF RADAR) MF RADAR
IS/THOMSON SCATTER-VHF/UHF-RADAR

A-02

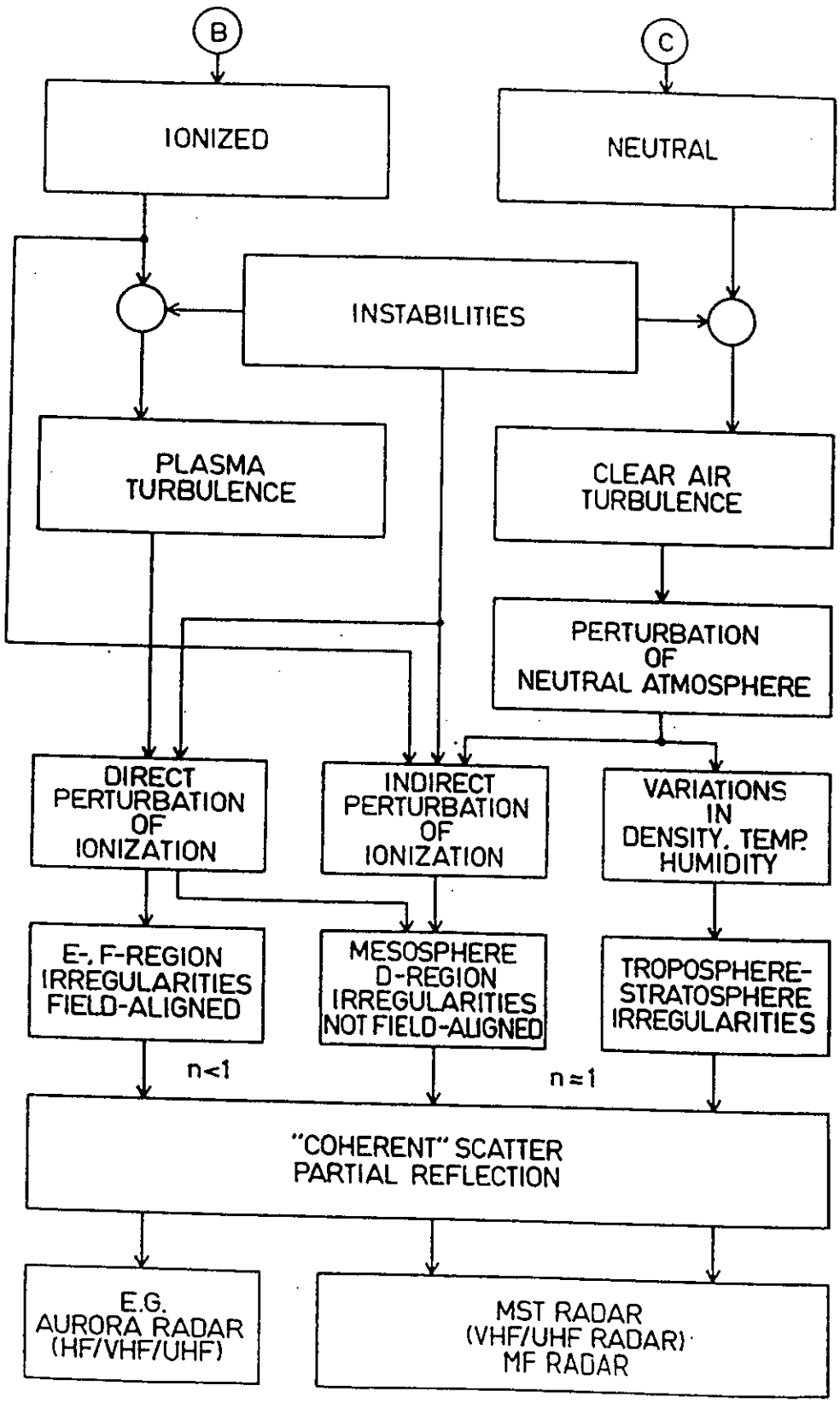
B
C
IONIZED
NEUTRAL
INSTABILITIES
PLASMA TURBULENCE
CLEAR AIR TURBULENCE
PERTURBATION OF NEUTRAL ATMOSPHERE
DIRECT PERTURBATION OF IONIZATION
INDIRECT PERTURBATION OF IONIZATION
VARIATIONS IN DENSITY, TEMP. HUMIDITY
E-, F-REGION IRREGULARITIES FIELD-ALIGNED
MESOSPHERE D-REGION IRREGULARITIES NOT FIELD-ALIGNED
TROPOSPHERE-STRATOSPHERE IRREGULARITIES
n<1
n≈1
"COHERENT" SCATTER PARTIAL REFLECTION
E.G. AURORA RADAR (HF/VHF/UHF)
MST RADAR (VHF/UHF RADAR) MF RADAR

A03

RADAR METHODS FOR INVESTIGATIONS OF THE LOWER AND MIDDLE ATMOSPHERE AND THE THERMOSPHERE/IONOSPHERE

Typical operation parameters (approximate)

Radar Method	Frequency Range	Wavelength in m	Average Power in kW	Antenna Dimension in wavelengths	Height Region
MF Radar	MF-HF	150-50	0.01-1	1-10	M,LT/Io
HF Radar *	HF	300-10	0.01-5	0.5-1	Th/Io
Coherent Radar ^	HF-VHF	30-1	0.1-1	5-50	Th/Io
Meteor Radar	HF-VHF	10-6	0.1-10	2-10	M,LT
MST Radar	VHF	6-7	1-100	5-50	M,S,T
Incoherent Scatter Radar	VHF-UHF	6-0.25	100-300	100-300	M,LT/Io
ST Radar	VHF-SHF	6-0.1	1-500	10-500	S,T
BL Radar	UHF	0.3	0.01-0.1	10	T

MF = 0.3-3.0 MHz
HF = 3.0-30 MHz
VHF = 30-300 MHz
UHF = 300-3000 MHz
SHF = 3-30 GHz
* = Ionosonde

M = Mesosphere
S = Stratosphere
T = Troposphere
LT = Lower Thermosphere
Th/Io = Thermosphere/Ionosphere
^ = Irregularity Scatter

A01

HF Radar High Frequency Radar

(1) Ionosondes

Total reflection of radar waves in the ionosphere occurs when the radar frequency is equal to the plasma frequency. Using vertically beaming radar antennas, the ionospheric electron density profile is measured. Applying suitably low radar frequencies and sufficiently large radar power, the lower E- and upper D-region electron density profiles can be measured, too. Ionosondes had been the traditional instruments to deduce the electron density of the ionosphere. The modern systems are for instance known as Digisondes or Dynasondes, which are also applied in the same way as the MF radars. These are also used in the Doppler and spaced antenna mode to measure velocities.

(2) 'Coherent' HF radar

Using ionosondes with oblique beam ground-backscatter as well as 'coherent' backscatter from ionospheric irregularities in the E- and F-region is measured. Applying directional antennas and measuring the Doppler shift allows deduction of ionospheric velocities at larger ranges. This method is not suitable for studying the D-region (mesosphere).

A05

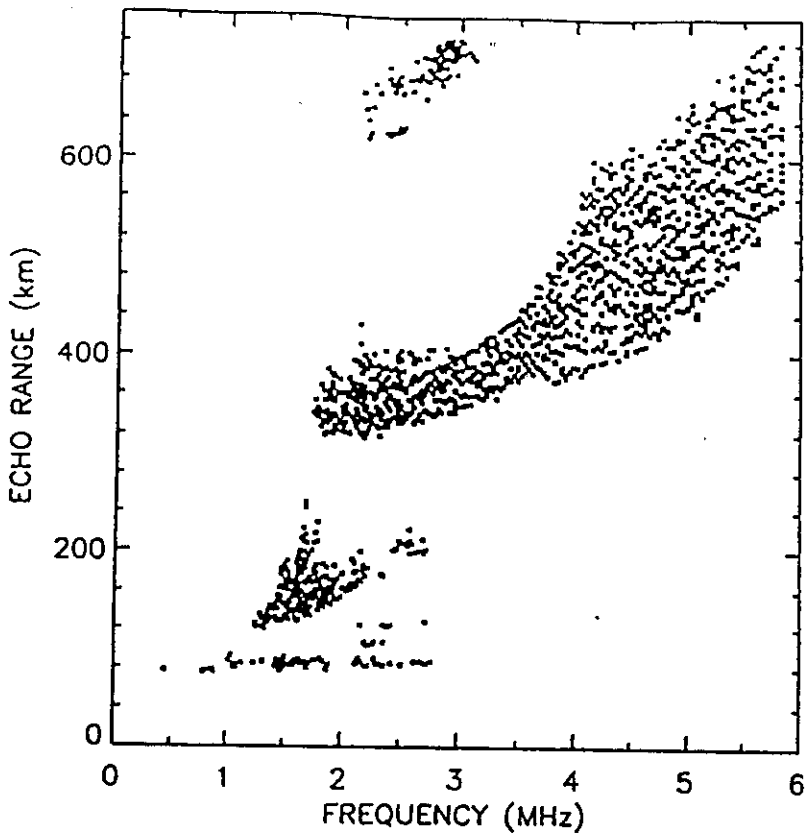
ECHO RANGE (km)
0
200
400
600
0
1
2
3
4
5
6
FREQUENCY (MHz)

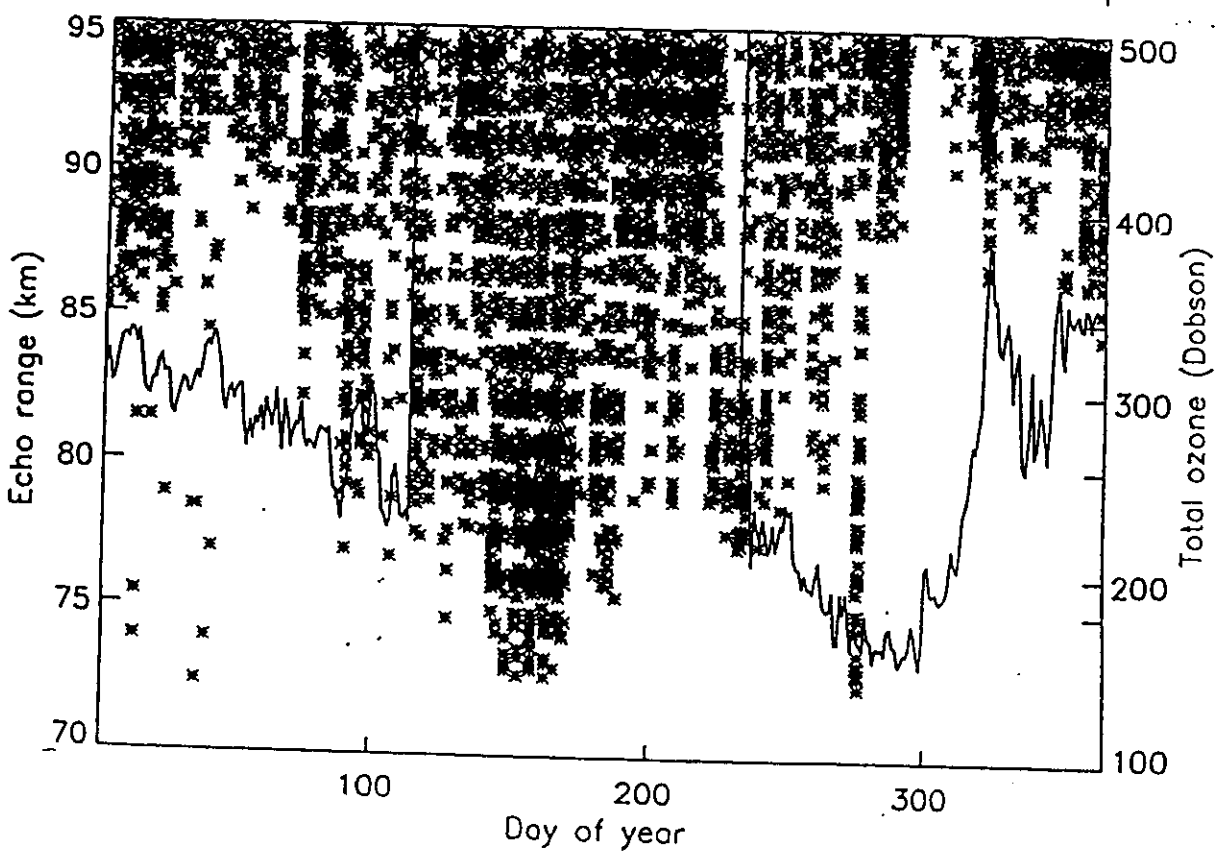
Echo range (km)
95
90
85
80
75
70
100
200
300
Day of year
500
400
300
200
100
Total ozone (Dobson)

'Coherent' Radars

These are radars operating with oblique beam to illuminate ionospheric irregularities in the E- and F-region, which are aligned parallel to the Earth's magnetic field. Many of such radars, operated particularly around 50 MHz and 150 MHz, have been specifically designed and operated to study these plasma irregularities and the ionospheric dynamics. Their name stems from the discrimination of the scattering process from incoherent scatter. However, a better name would be for instance: 'Ionospheric irregularity scatter radars'. This is not the special subject of this lecture, but also VHF MST radars have been applied for the purpose of studying the ionospheric irregularities.

The scattering process is highly aspect sensitive (i.e. the scatter cross section decreases rapidly when the radar beam points off the perpendicular direction with respect to the Earth's magnetic field). Such studies are, thus, particularly convenient at the magnetic equator, since the MST radars are usually pointing close to the vertical direction, i.e. perpendicular to the magnetic field at the equator. Also MST radars at mid-latitudes have been applied for such investigations. Scatter cross sections, drift velocities of the scattering irregularities and aspect sensitivity was for instance measured with these modified MST radars.

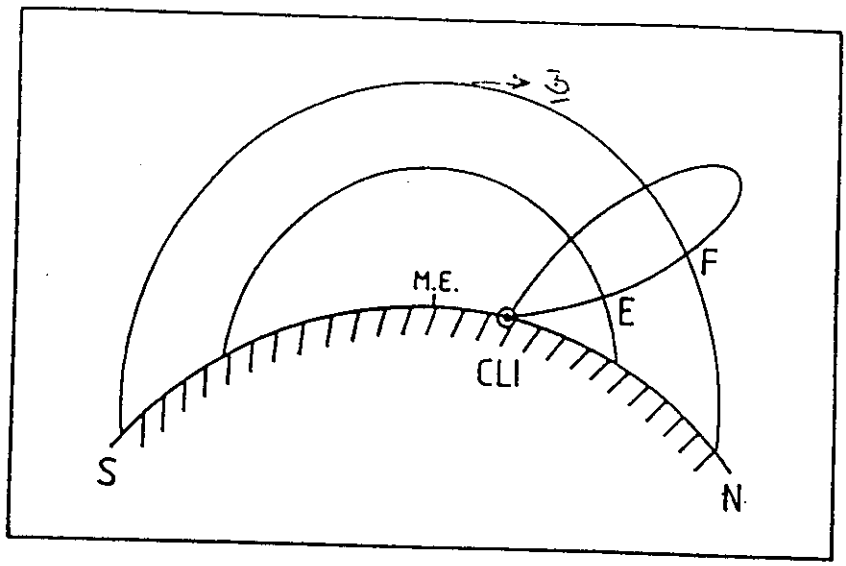

Fig. 1 Schematic view of the Chung-Li radar beaming northward to meet perpendicularity to the Earth's magnetic field in the E- and F-region. M.E. indicates magnetic equator.

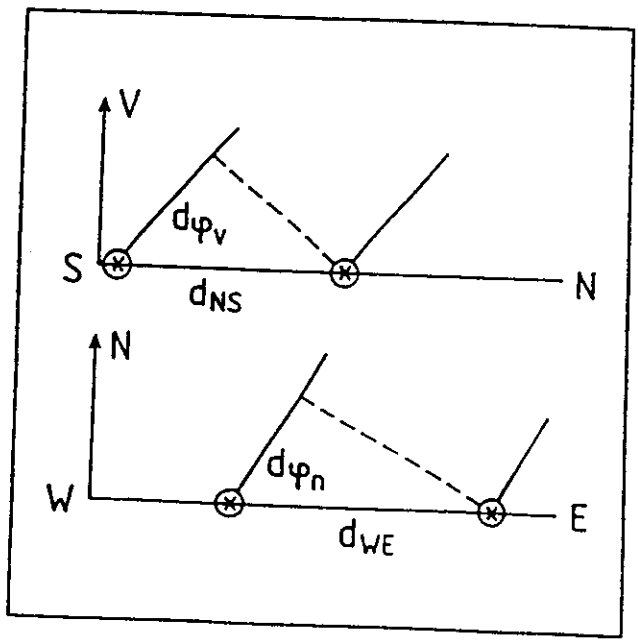

A04

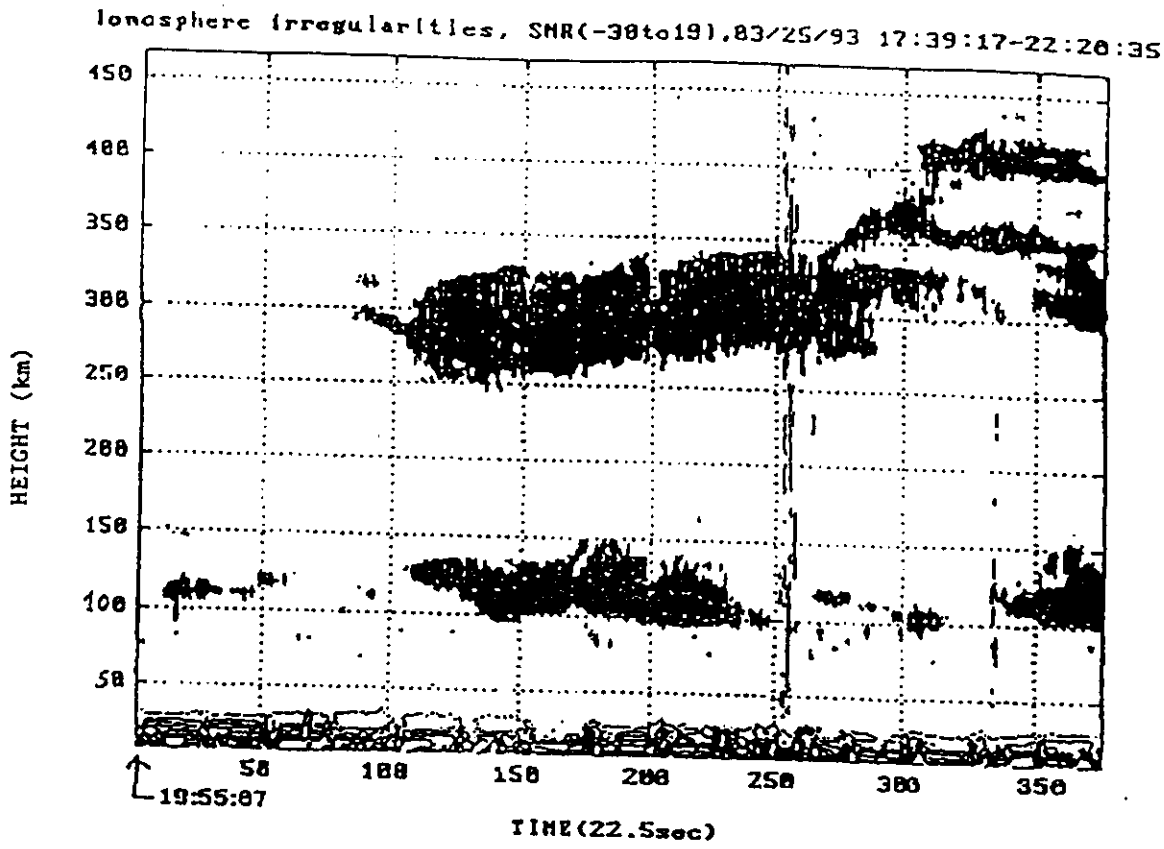

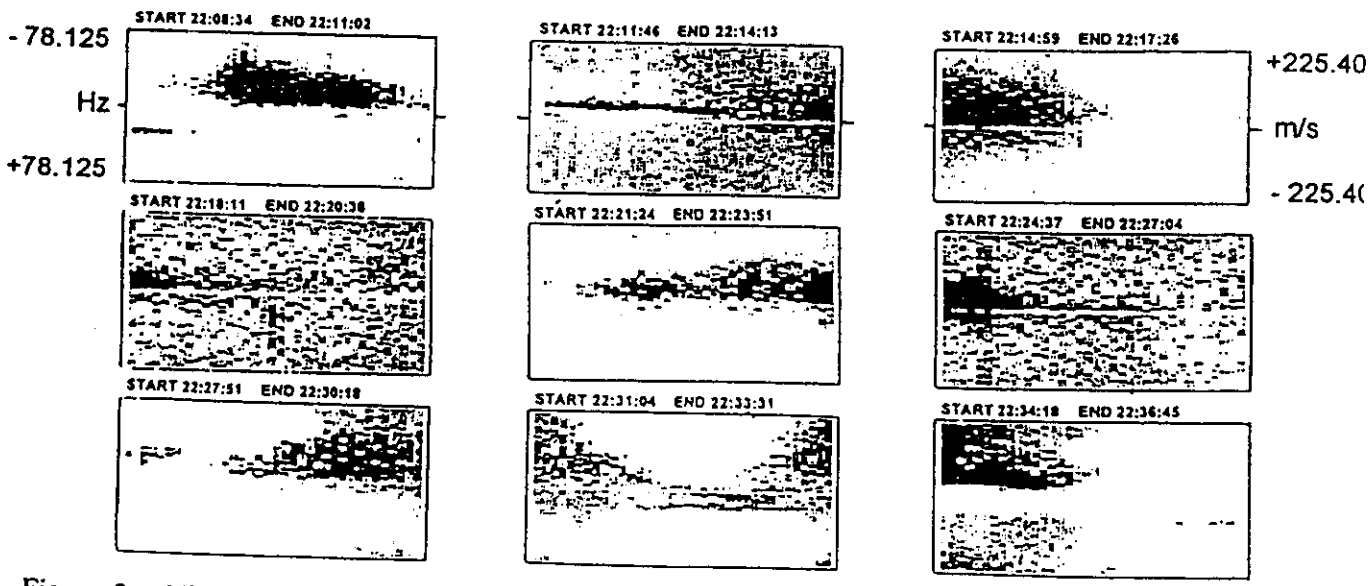

Figure 2. Nine spectrograms started at 22:08:34 LT and ended at 22:36:45 LT with a same time interval of 147.5 seconds at the same range gate of 107 km altitude. The vertical axis of each panel represents the radial Doppler shift in Hz (also the Doppler velocity in m/s) and the horizontal axis represents time.

A09

MF Radar Medium Frequency Radar

(1) The MF radar signal is partially reflected from gradients or irregularities in the D-region electron density profile (the D-region is the ionized part of the mesosphere). It is used in the partial reflection mode to measure electron density profiles in the D-region with the differential absorption experiment (DAE) and the differential phase experiment (DPE): The ordinary and extra-ordinary wave undergo different attenuation and partial reflection depending on electron density, direction to the Earth magnetic field and the neutral-electron collision frequency (neutral density). For these measurements the application of orthogonal polarizations of the radar signal is needed.

(2) The MF radars are also used in the spaced antenna mode to measure horizontal velocities in the mesosphere and lower thermosphere. This technique is now frequently applied for studies of the dynamics of this region. For this measurement a set of three receiving antennas is needed.

A1

$$A_{O,\,x} \approx R_{O,\,x}\ \exp\left(2\frac{\Omega}{c}\int_0^h n_{O,\,x}\,dh\right)$$

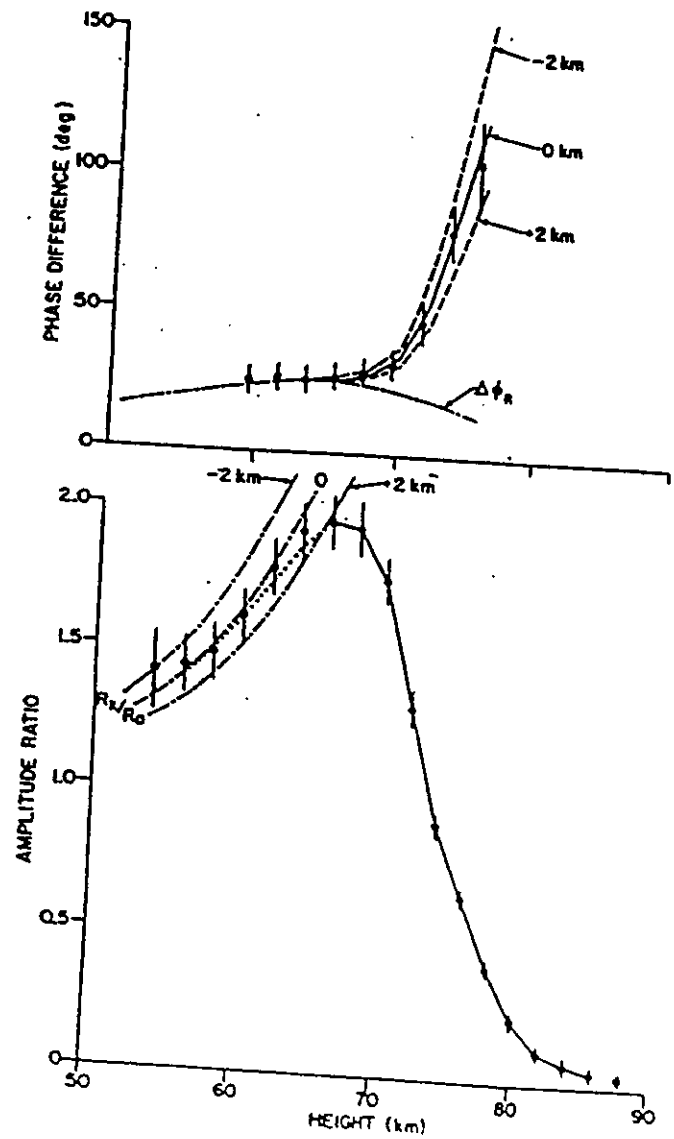

Meteor Radar

Meteors coming in from space ablate as they encounter the lower thermosphere and upper mesosphere and produce ionized trails. Radar waves are scattered or reflected from these trails, depending whether the electron density in the trail is underdense (plasma frequency smaller than radar frequency) or overdense (plasma frequency larger than radar frequency), respectively. The amplitude of the underdense echo rises rapidly and decays exponentially since diffusion causes the trail to expand. Since the trail is carried with the neutral wind, the radar signal experiences a Doppler shift. By measuring this Doppler shift, the wind velocity can be determined. The decay time of the signal yields the diffusion coefficient.

The radar measurements have to be carried out with directional antennas or in the interferometer mode to determine the location of the meteor trail.

MST radars can also be used in the meteor radar mode, either mono-static or bi-static.

Echoes from the high electron density surrounding the meteor head can also be observed with very powerful IS radars.

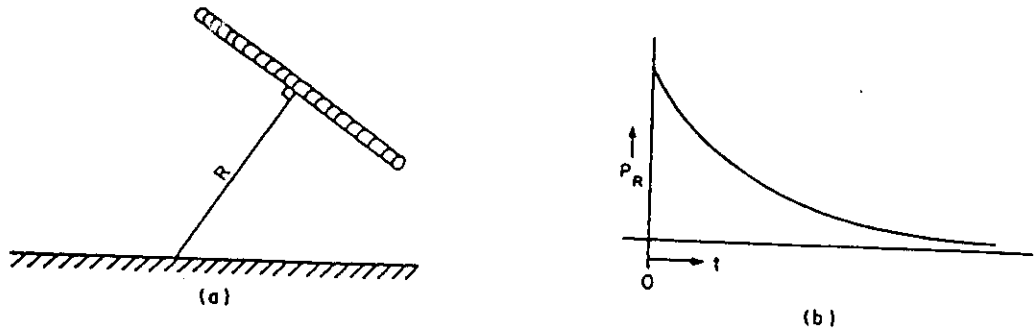

Low-density long-wavelength reflections.

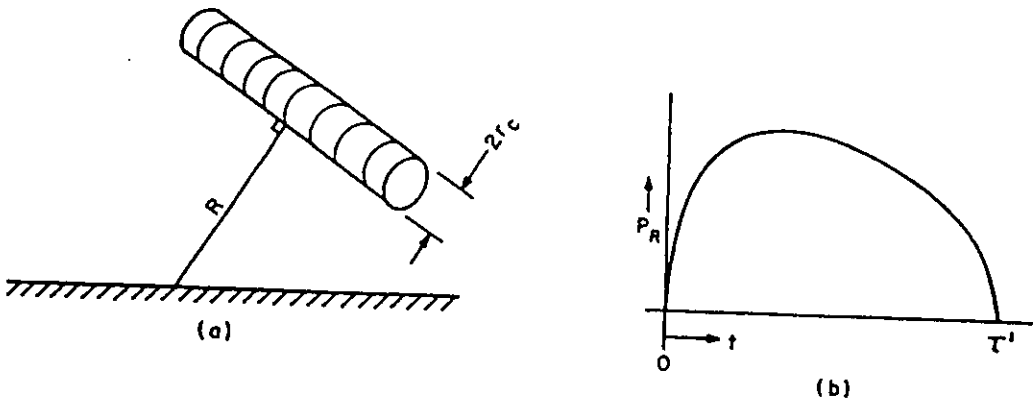

High-density long-wavelength reflections.

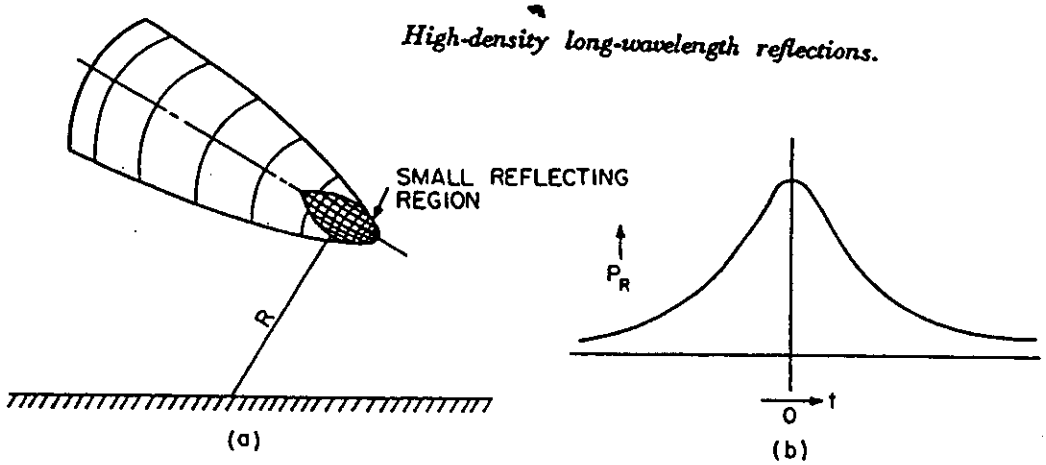

Low-density short-wavelength reflections.

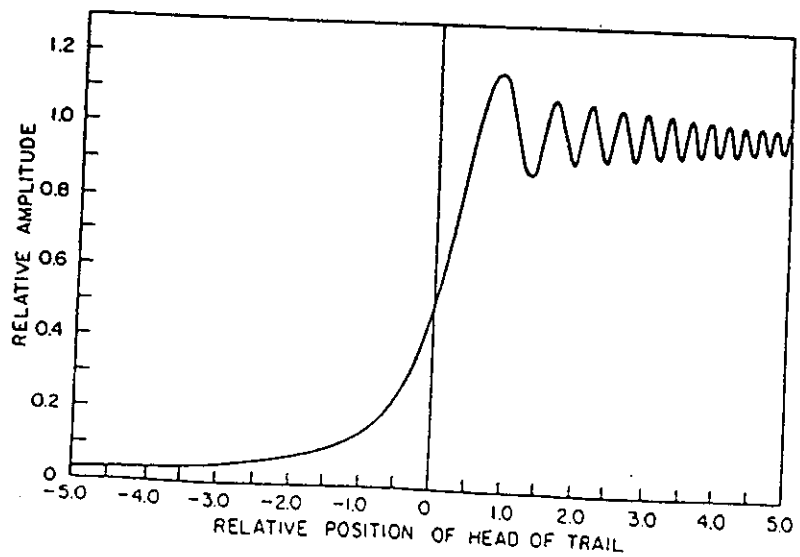

Amplitude variation of

IS Radar (ISR) Incoherent Scatter Radar

When the plasma frequency in the ionosphere is smaller than the radar frequency, free electrons in the ionosphere act as Thomson scatterers, and the scattered waves from all electrons in a unit volume superimpose randomly due to the thermal motions of the electrons. Since the electrons are part of the ionospheric plasma, the ions particularly control the scattering process. In the middle atmosphere the collisions between neutral particles and ionospheric particles are non-negligible and the scattering process is collision-dominated. The scatter cross section of incoherent scatter is very small, and therefore high power-aperture radars are needed. Due to restrictions given by plasma parameters and by the sky noise level, the usable frequency range for IS radars is between about 50 MHz and 1 GHz. Optimum frequencies are around 400 to 500 MHz.

In the collision-dominated scattering regime, i.e. in the mesosphere and lower thermosphere, the electron density, ion drift (neutral) velocity, temperature and neutral density, the negative ion density and the ion mass can be measured.

Typical range resolution of 1 km and time resolution of 1 minute can be achieved.

A1

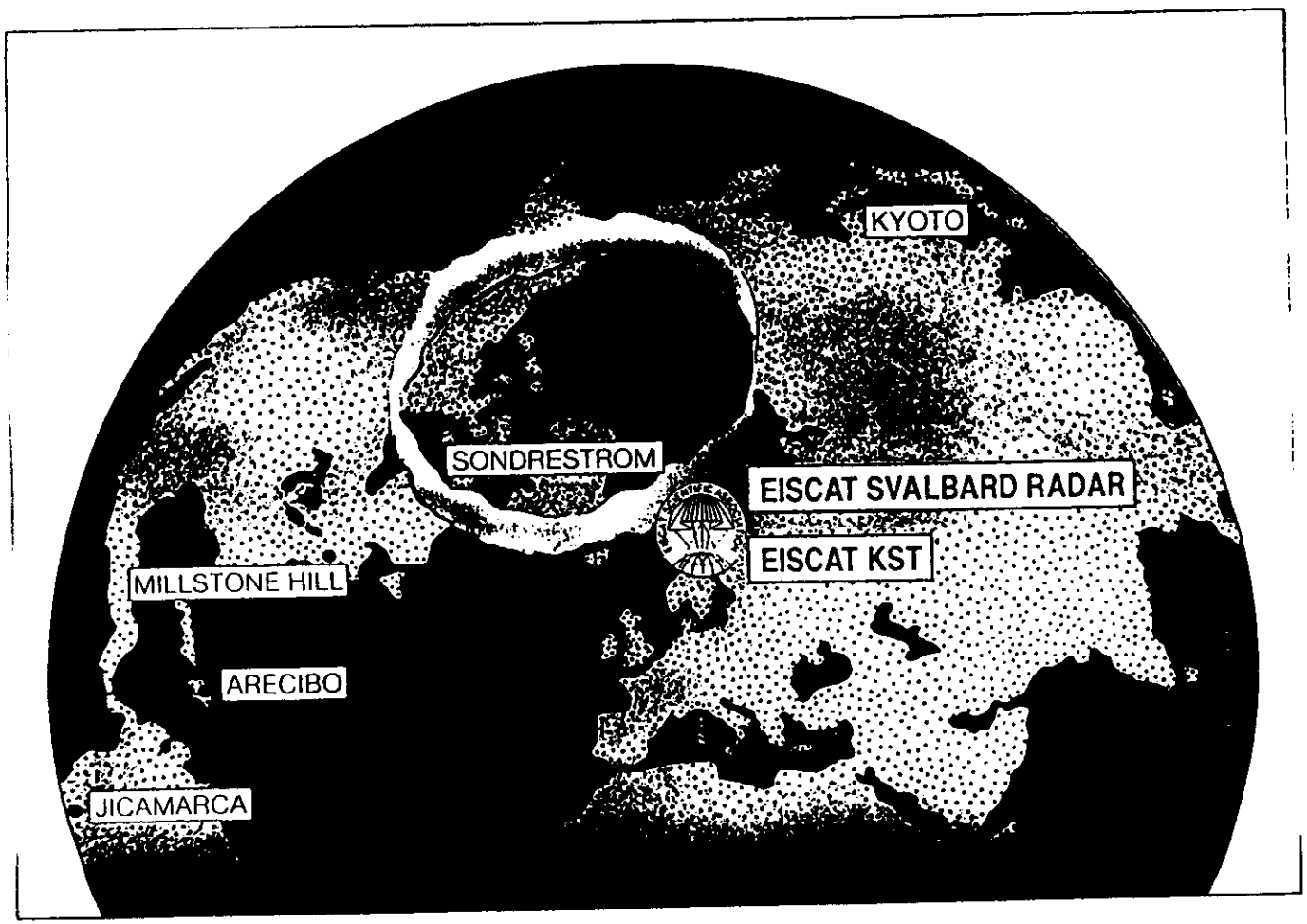
KYOTO
SONDRESTROM
EISCAT SVALBARD RADAR
EISCAT KST
MILLSTONE HILL
ARECIBO
JICAMARCA

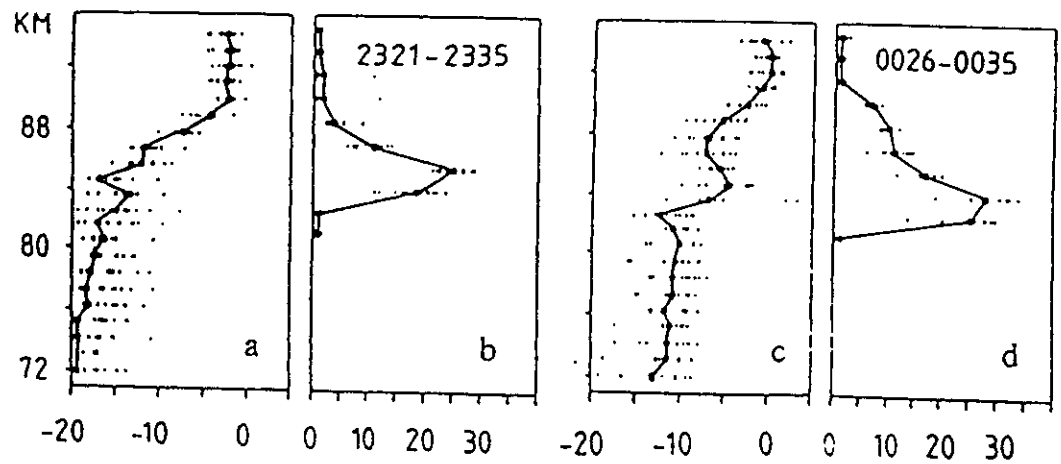

Fig. 11 Profiles of scattered power observed with the EISCAT UHF radar (a, c), and the CUPRI VHF radar (b, d) on 1/2 July 1988; after /33/.

Particular coherent scatter during PMSE

Whereas the incoherent scatter results from independent electrons in thermal equilibrium (thermal scatter), in particular conditions of large cluster ions and other contaminants in the mesopause region, the incoherent scattering process is changed substantially and this process can be called non-thermal scatter. The signal exhibits a highly coherent nature and exceeds the common incoherent and turbulence scatter level by many orders of magnitude.

These Polar Mesosphere Summer Echoes (PMSE), occurring in the very cold high-latitude mesopause due to the formation of ion clusters and ice particles, should not be confused with the usual MST radar echoes from turbulence induced irregularities in the D-region/mesosphere.

Although the difference to the conventional incoherent and turbulence scatter from the mesosphere is commonly agreed upon, this process, occurring during so-called PMSE conditions is not fully understood yet.

Hoppe et al.: Polar Mesospheric Backscatter at 224 MHz

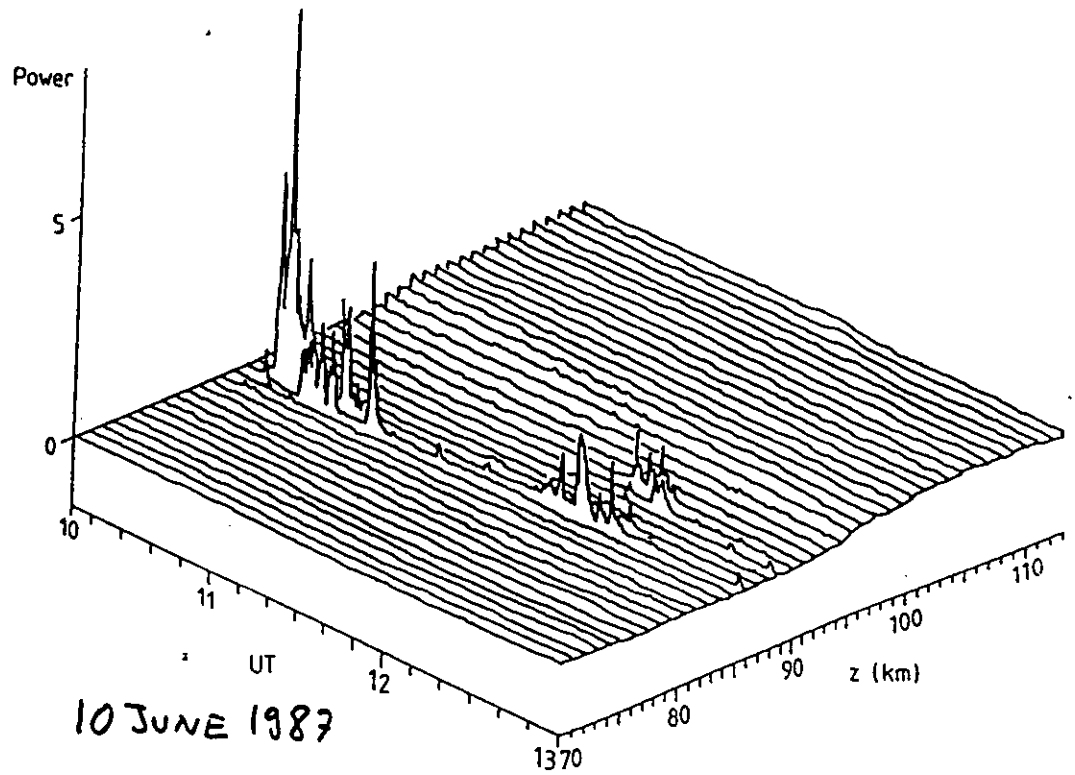

A K

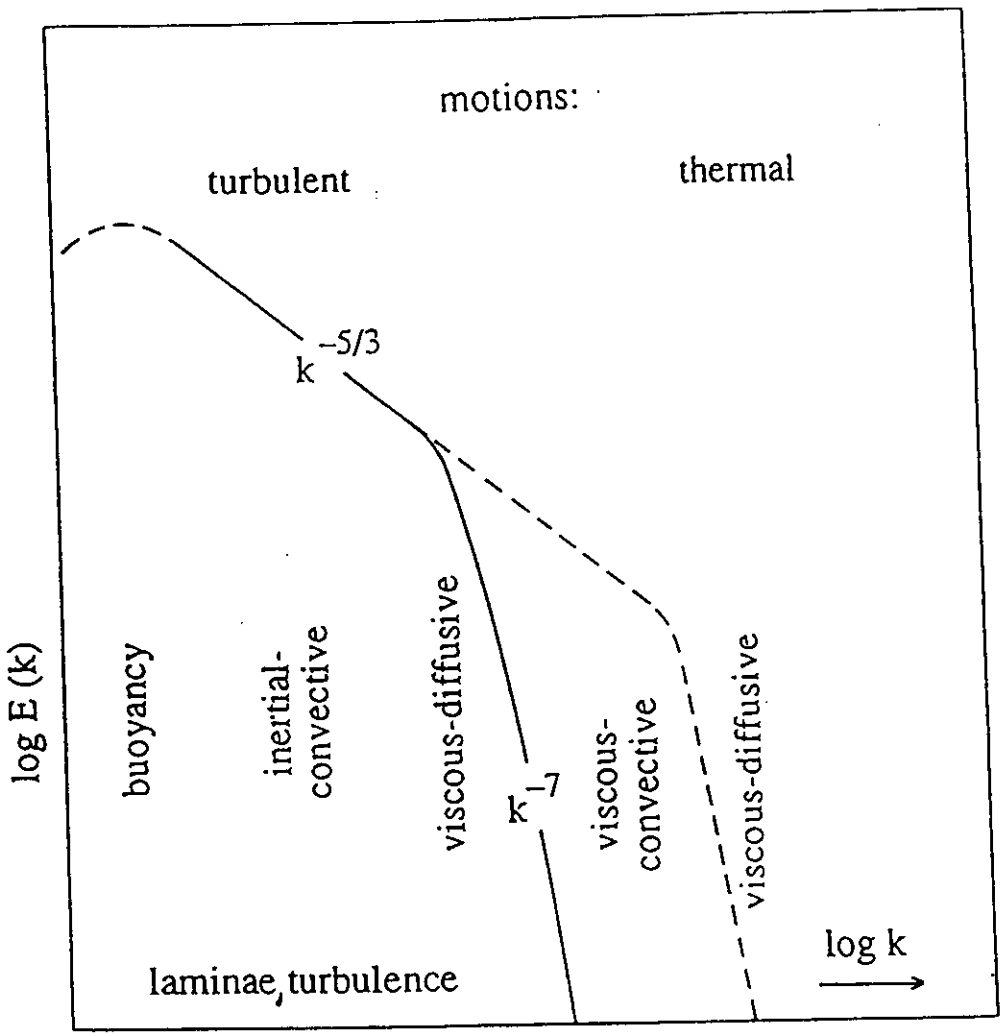

(after Kelley et al., 1987)

Total backscattered power P_s

$$P_s = \frac{\alpha_e^2 \, A_e \, P_t \, \Delta r}{4\pi \, r^2} \cdot \sigma$$

The total scatter cross section is
in the mesosphere and lower thermosphere

$$\sigma = \sigma_t + \sigma_i$$

Depending on many, partially related, parameters

the scatter cross section for **MST**: σ_t

or the scatter cross section for **ISR**: σ_i

may dominate
and there is a transition region between both.

We will try to explain why this is the case and how one can discriminate between these components.

A-2

Scatter cross section of incoherent (Thomson) scatter:

$$\sigma_i = N_e \, \sigma_e$$

$$\sigma_e = 4 \, \pi \, r_e \left(\frac{\alpha^2}{1 + \alpha^2} + \frac{1}{(1 + \alpha^2) \cdot (1 + T_e / T_i + \alpha^2)} \right)$$

$$\alpha = \frac{\lambda}{2 \, \pi \, \lambda_D}$$

$$\lambda_D = 69 \cdot \left(\frac{T_e}{N_e}\right)^{1/2}$$

N_e = number density of free electrons

T_e = electron temperature,
assumed to be equal to ion temperature
and neutral temperature in the mesosphere

r_e = classical radius of electron (acting as
an individual 'Thomson scatterer' with
cross section of $0.998 \cdot 10^{-28}$ m^2)

λ_D = Debye length (ions forming a shielding
sphere around electron of radius λ_D)

The refractive index variations in the atmosphere are related to random irregularities generated by turbulence, or to steep gradients introduced by horizontal layering or structuring of the atmosphere. The refractive index variations are directly related to variations of the atmospheric parameters: humidity, temperature, pressure (corresponding to air density) and electron density. The refractive index for the troposphere, stratosphere and mesosphere (ionospheric D-region) at VHF and UHF is:

$$n = 1 + \left(77.6 \frac{p}{T} + 3.75 \cdot 10^5 \frac{e}{T^2} \right) \cdot 10^{-6} - 40.3 \frac{N_e}{f_o^2}$$

where e is the partial pressure of water vapor (humidity) in mb, p the atmospheric pressure in mb, T the absolute temperature in Kelvin, N_e is the ionospheric electron density in m^{-3}, and f_o the radar operating frequency in Hz.

M.ST

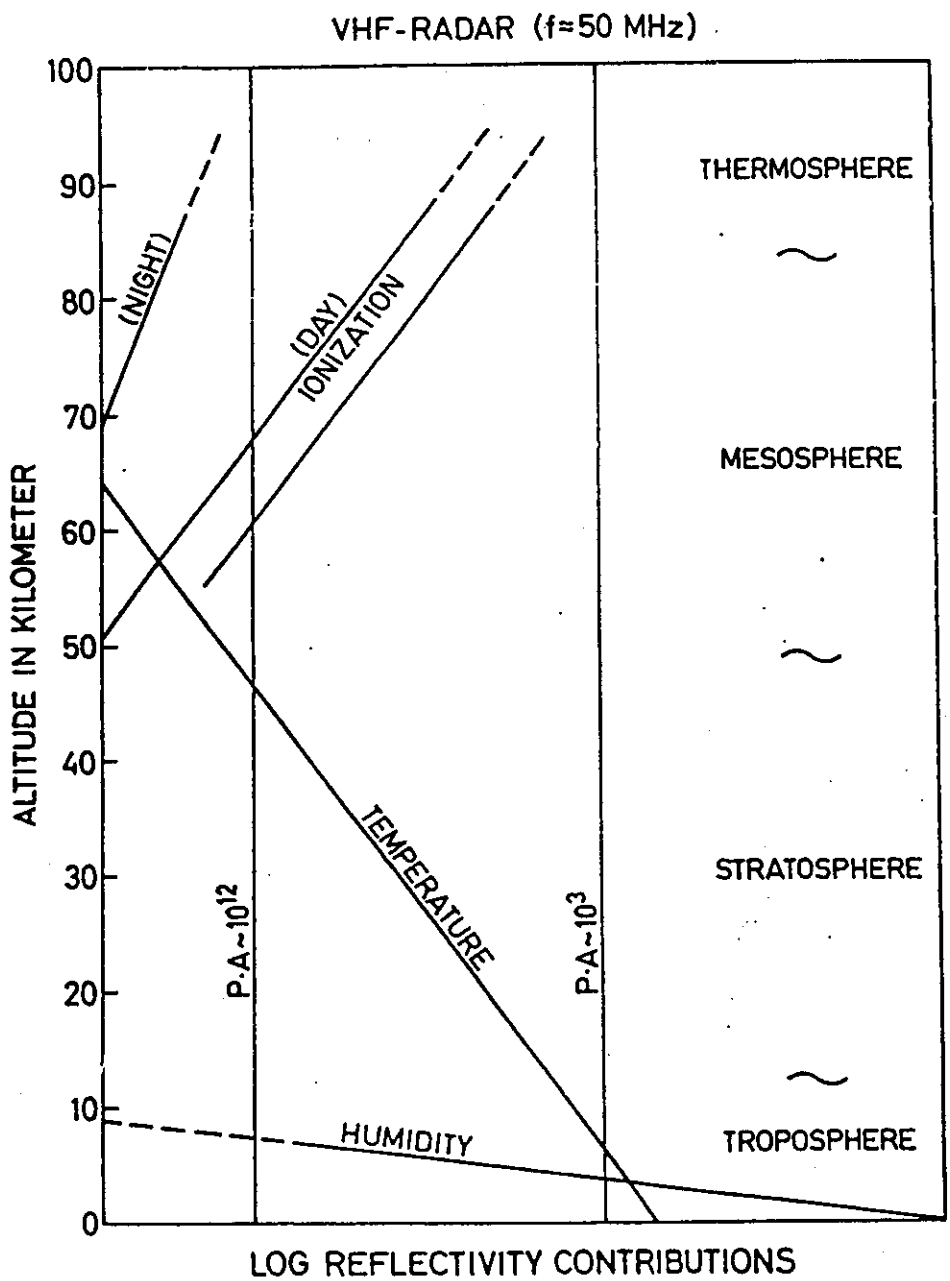
VHF-RADAR (f=50 MHz)
100
90
80
70
60
50
40
30
20
10
0
ALTITUDE IN KILOMETER
(NIGHT)
(DAY) IONIZATION
TEMPERATURE
HUMIDITY
P.A.~10^12
P.A.~10^3
THERMOSPHERE
MESOSPHERE
STRATOSPHERE
TROPOSPHERE
LOG REFLECTIVITY CONTRIBUTIONS

The radar reflectivity η which is the cross section σ_t per unit volume at the wavelength λ for pure volume scattering from isotropic turbulence in the inertial subrange:

$$\eta = \text{const} \cdot C_n^2 \, \lambda^{-1/3}$$

This relation (const = 0.4) hold only for radar wavelengths which are larger than the inner scale of the inertial subrange of turbulence fluctuations. This inner scale depends on turbulence intensity and the kinematic viscosity. The latter increases as a function of altitude, which places a lower limit to radar wavelengths which can be used to detect echoes from the middle atmosphere. For scatter from fluctuations in the viscous subrange, which result from fluctuations of neutral turbulence an unified and appropriate formalism to determine η is not available yet, since the dependency on background gradients of the other parameters is not quite solved so far.

When atmospheric turbulence or other small scale perturbations in the electron gas in the mesosphere mixes the vertical profile of the refractive index and the associated gradients, fluctuations of n result, which in turn cause scattering and reflection of radar waves. It is useful to define a refractive index structure constant C_n^2 which is related to the mean square fluctuations $<dn^2>$ of the refractive index by

$$C_n^2 = a <dn^2> L_o^{-2/3},$$

where a is a constant ($\simeq$ 5) and L_o is the outer scale of turbulence in the inertial subrange, which is proportional to the square root of turbulence energy dissipation rate ϵ and the -3/2 power of the buoyancy frequency ω_B of the atmosphere.

The turbulence refractive index structure constant can be expressed as:

$$C_n^2 = 0.7\ \epsilon^{2/3}\ M^2\ \omega_B^{-2}\ F^{1/3}$$

Here F is the filling factor, i.e. the relative portion of the scatter volume which is filled with turbulence irregularities, and M the generalized potential refractive index gradient.

For the unionized atmosphere we find for the troposphere, where the humidity e is not negligible (specific humidity q = e / 1.62 p):

$$M_t = -79 \cdot 10^{-6} \frac{p}{T^2} \left(1 + 15.5 \cdot 10^3 \frac{q}{T} \right) \cdot \left(\frac{T \omega_B^2}{g} - \frac{7.8 \cdot 10^3}{\left(1 + 15.5 \cdot 10^3 \frac{q}{T} \right)} \frac{dq}{dz} \right)$$

for the stratosphere (humidity e is neglected):

$$M_s = -79 \cdot 10^{-6} \frac{p}{T^2} \frac{\omega_B^2}{g}$$

for the mesosphere (dominated by electron density N_e):

$$M_m = \frac{r_e \lambda^2}{2\pi} \left(N_e \left(\frac{\omega_B^2}{g} - \frac{d\rho}{\rho \, dz} \right) - \frac{dN_e}{dz} \right)$$

24

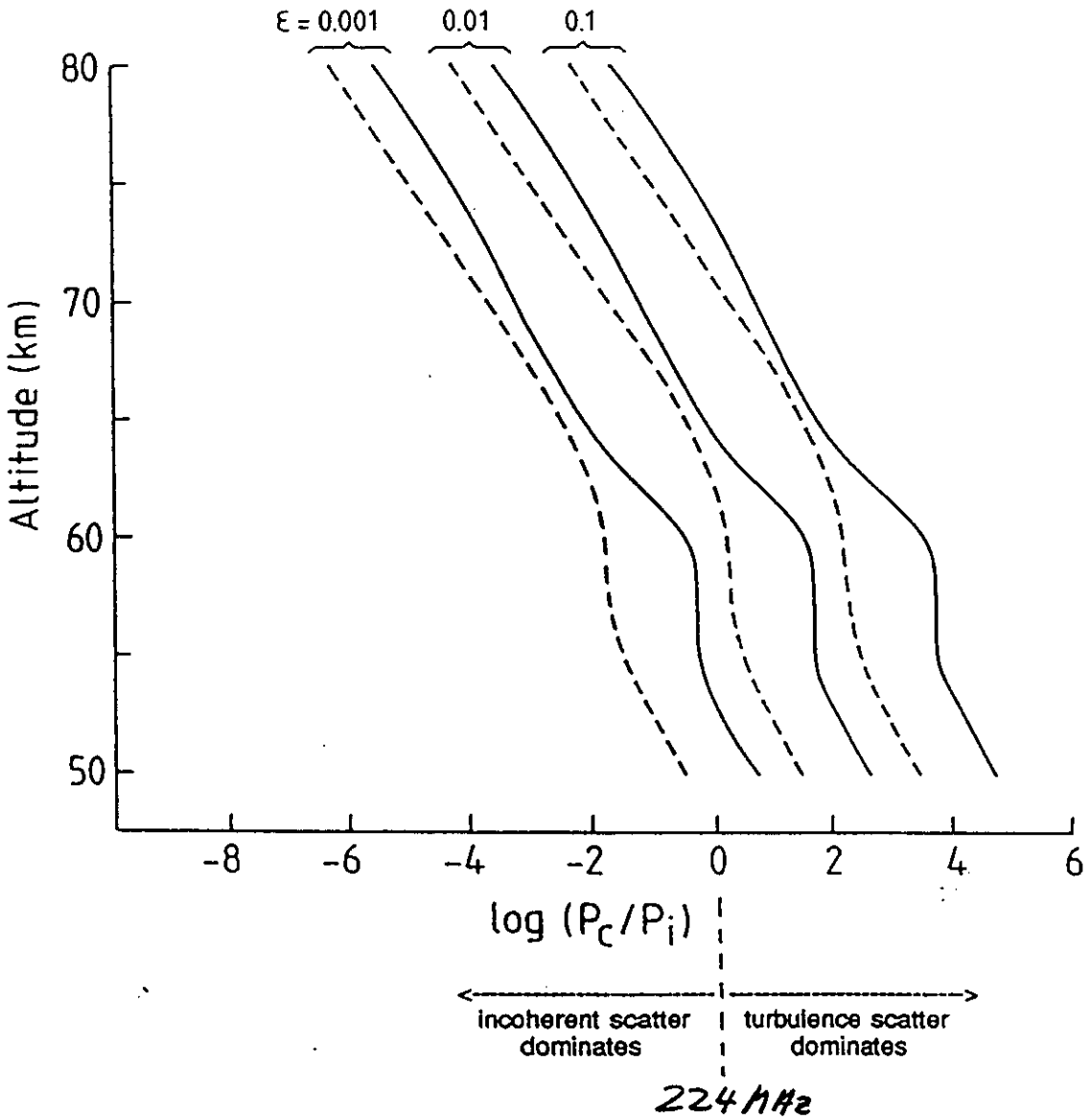

Figure 7. Calculated ratio of expected coherent (turbulence) backscatter power P_c to incoherent (Thomson) scatter power P_i as a function of altitude for two intervals from Figure 5. The three values of turbulent energy dissipation rate, ε W kg^{-1}, cover the range from weak (ε = 0.001) to strong (ε = 0.1) turbulence intensity.

$$F(\omega) \Leftrightarrow C(\tau) = A(\tau)\, \exp(i\varphi(\tau))$$

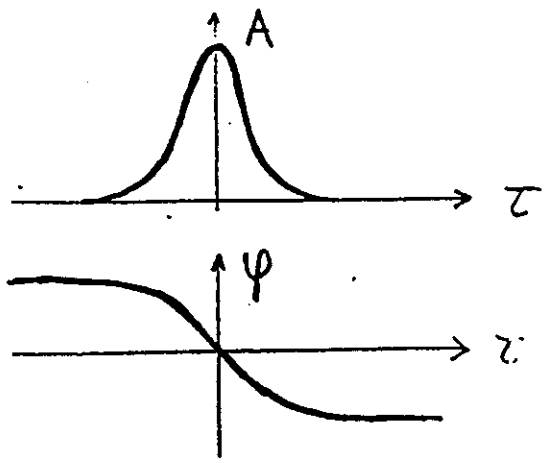

$$C(0) = \overline{E(0)\cdot E^{*}(0)} = P = A(0)$$

$$C'(0) = i\, m_1 \;\rightarrow\; \omega_d = \varphi'(0)$$

$$C''(0) = -m_2 \;\rightarrow\; \omega_s^2 = \frac{A'(0)}{A(0)}$$

$$F(\omega) = \frac{1}{2\pi} \int C(\tau) \exp(-i\omega\tau)\, d\tau$$

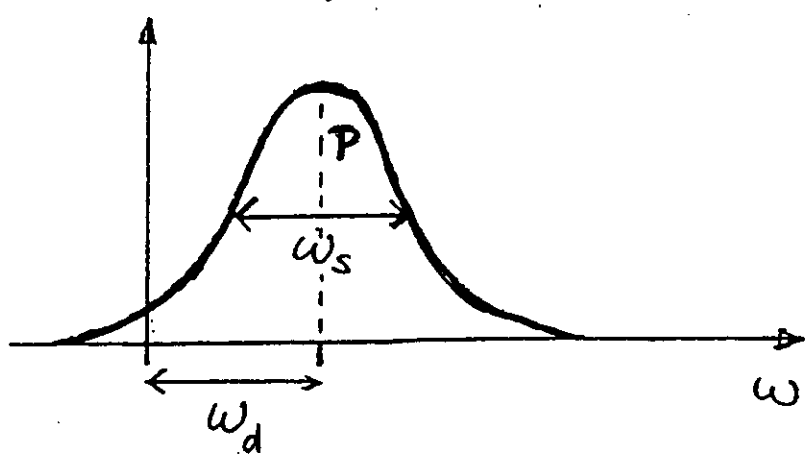

$$P = m_o = \int F(\omega)\, d\omega$$

$$\omega_d = \frac{m_1}{m_o}, \quad m_1 = \int \omega F(\omega)\, d\omega$$

$$\omega_s = \sqrt{\frac{m_2}{m_o} - \left(\frac{m_1}{m_o}\right)^2}, \quad m_2 = \int \omega^2 F(\omega)\, d\omega$$

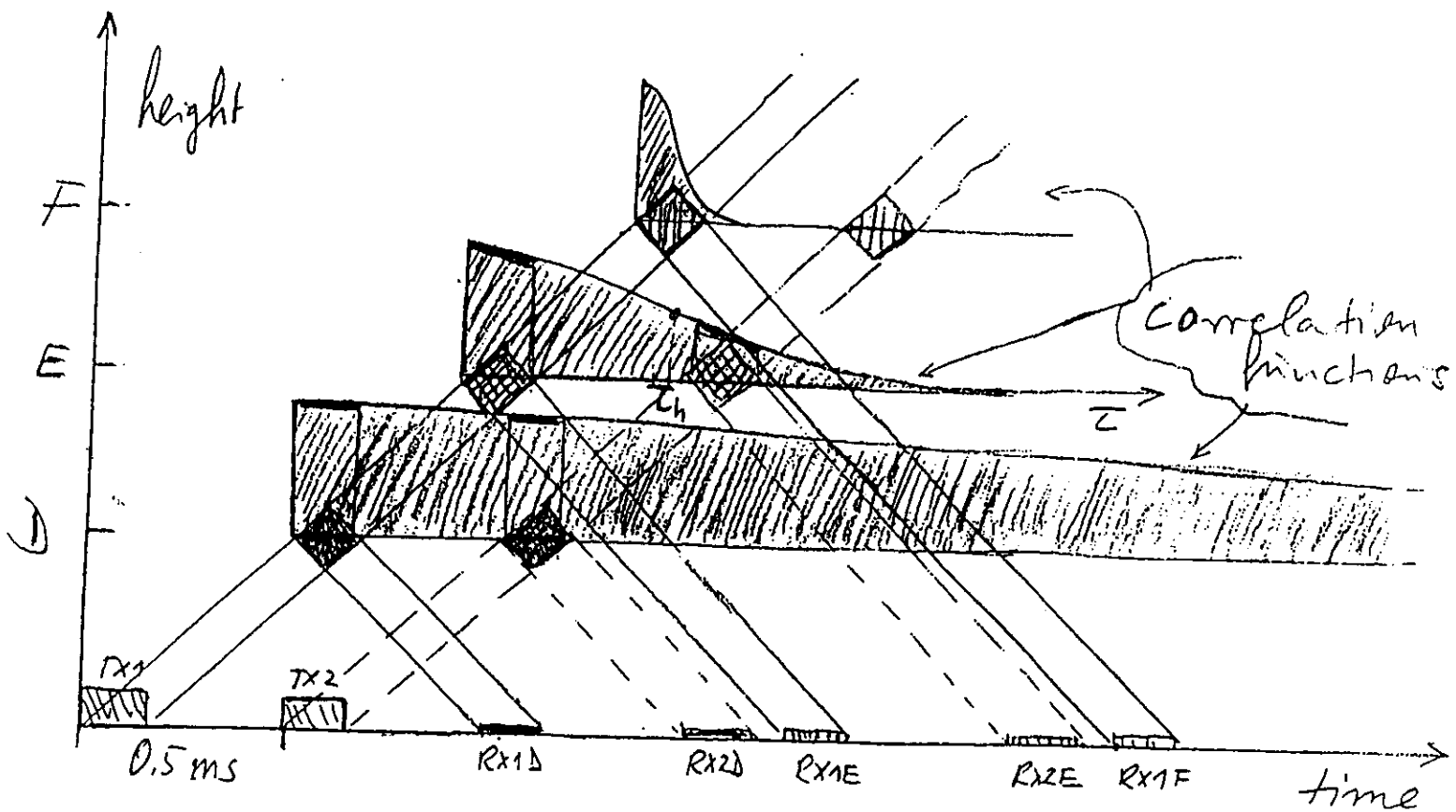
height
F
E
D
Tx1
Tx2
0.5 ms
Rx1D
Rx2D
Rx1E
Rx2E
Rx1F
time
correlation functions
τ_h
$\bar{\tau}$

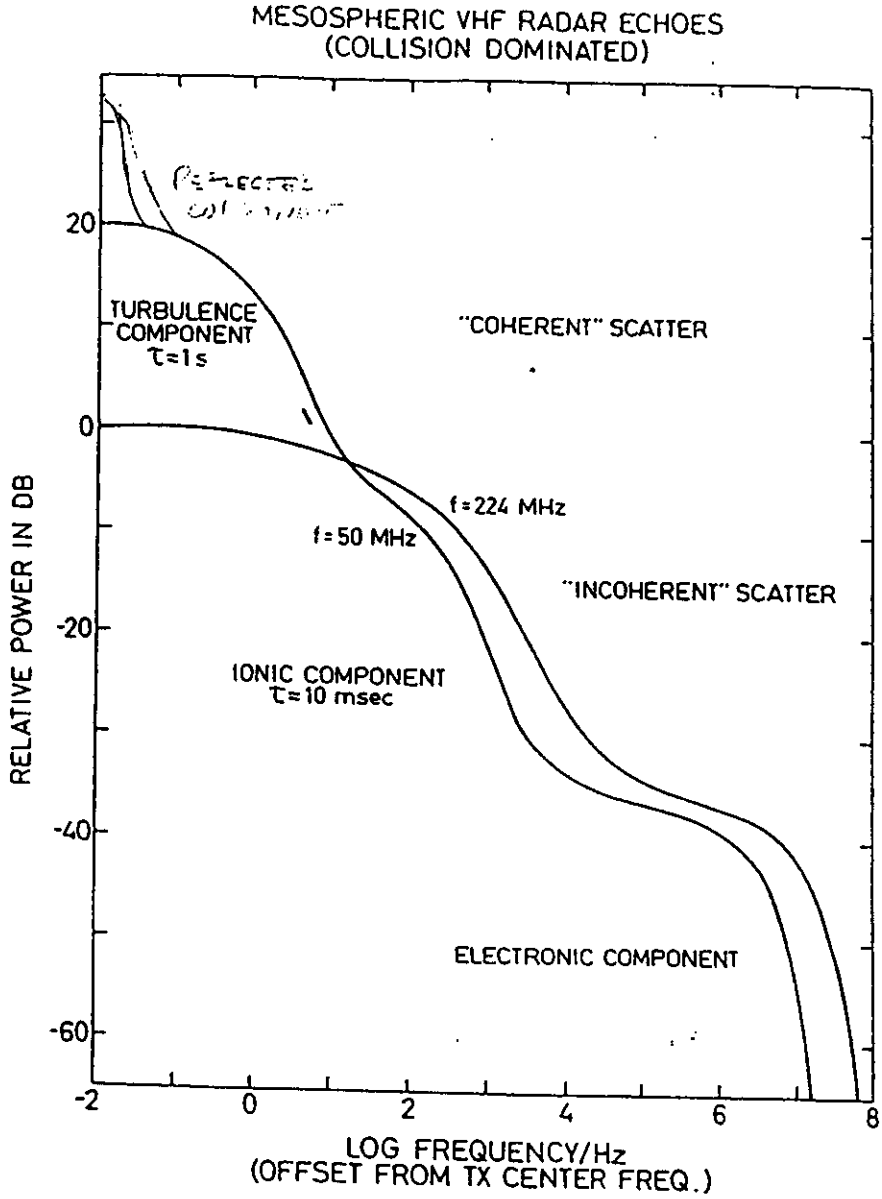
MESOSPHERIC VHF RADAR ECHOES
(COLLISION DOMINATED)
20
0
-20
-40
-60
-2
0
2
4
6
8
RELATIVE POWER IN DB
TURBULENCE
COMPONENT
τ=1 s
"COHERENT" SCATTER
f=224 MHz
f=50 MHz
"INCOHERENT" SCATTER
IONIC COMPONENT
τ=10 msec
ELECTRONIC COMPONENT
LOG FREQUENCY/Hz
(OFFSET FROM TX CENTER FREQ.)

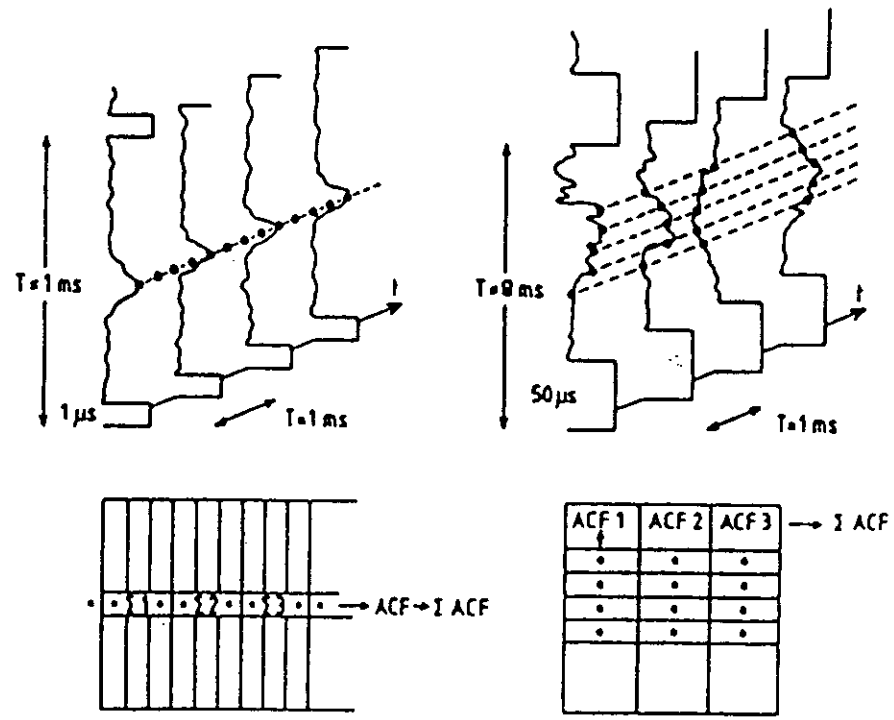

Figure 2. Range-time-amplitude diagrams for coherent (underspread) and incoherent (overspread) signals. The dots mark the sample points, which are used to compute autocorrelation functions ACF. The tables symbolize that for coherent signals coherent integrations ($\Sigma 1, \Sigma 2, \ldots$) are performed for fixed range gates over several interpulse periods, then the ACFs are computed which are finally accumulated (ΣACF). For incoherent signals the ACFs are computed within every interpulse period (ACF1, ACF2,...) and are then accumulated/integrated (ΣACF).

MST-RADAR

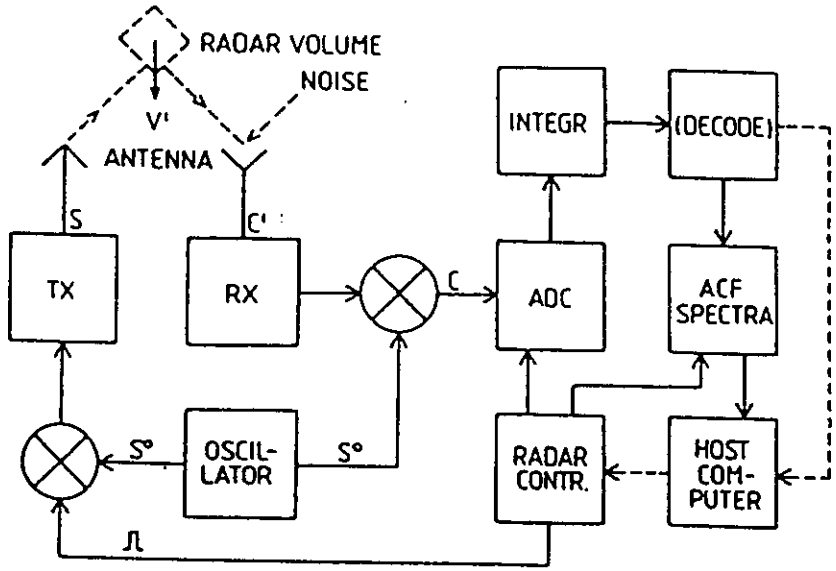

Figure 6a. Block diagram showing the basic configuration of an MST radar system (data acquisition for coherent signals).

IS-RADAR

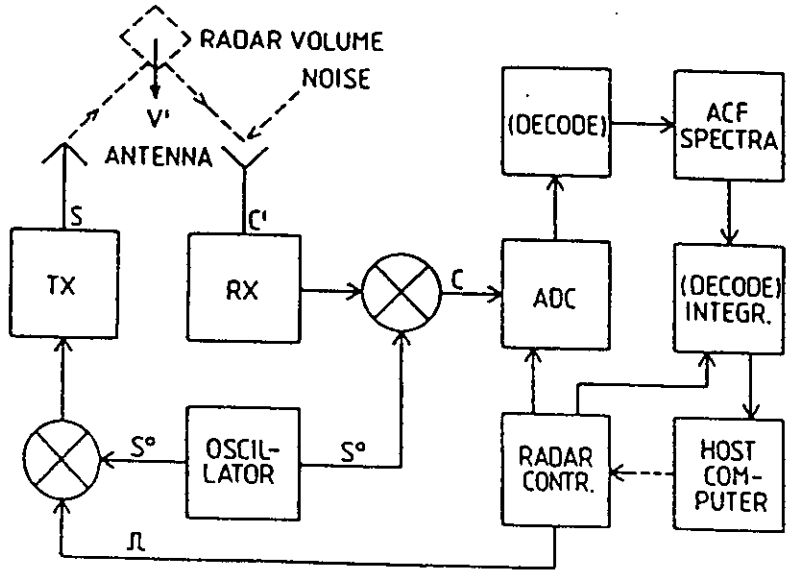

Figure 6b. Block diagram showing the basic configuration of an incoherent scatter radar system (data acquisition for incoherent signals).

A 32

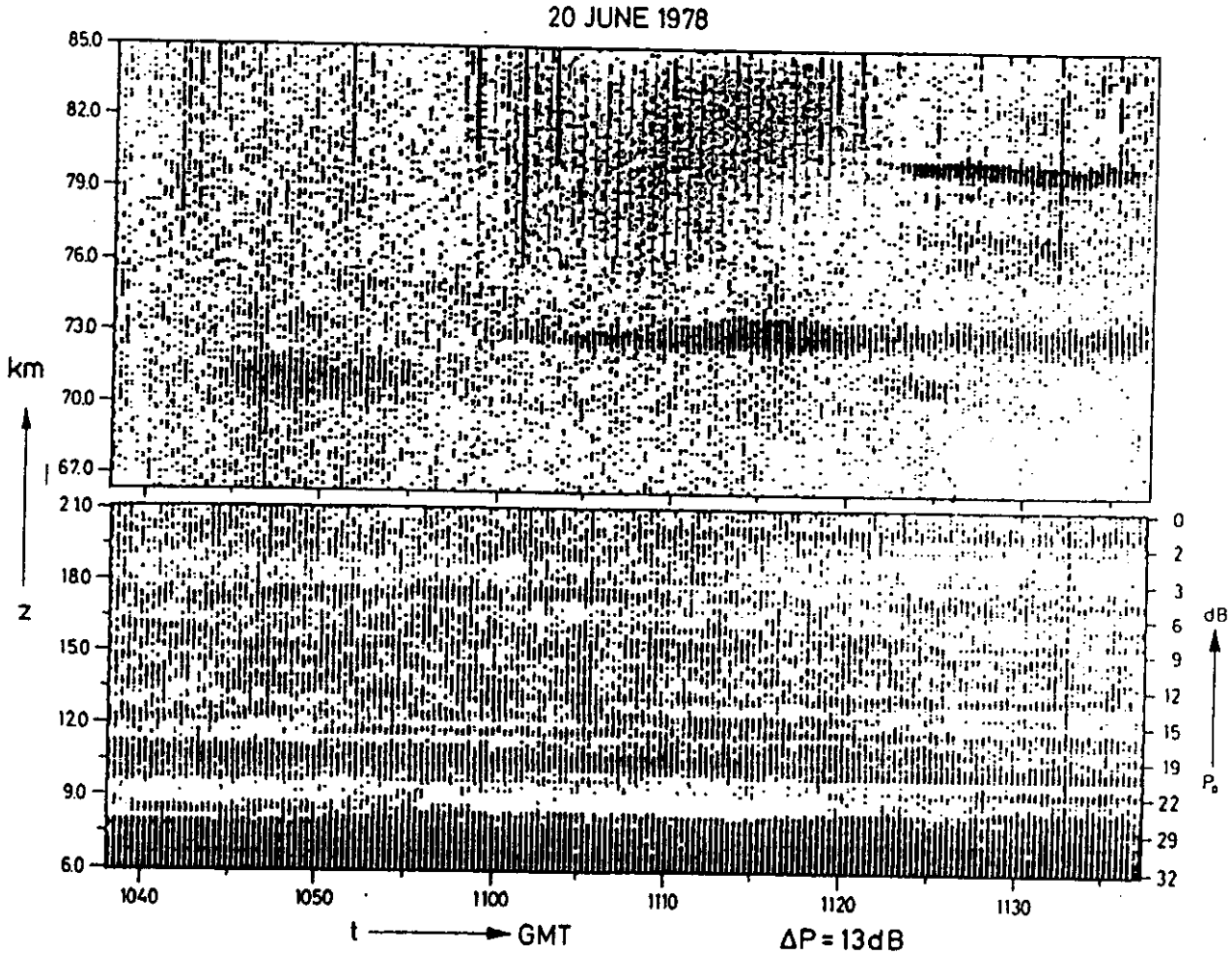
20 JUNE 1978
85.0
82.0
79.0
76.0
73.0
70.0
67.0
km
z
210
180
150
120
90
60
0
2
3
6
9
12
15
19
22
29
32
dB
P_a
1040
1050
1100
1110
1120
1130
t → GMT
ΔP = 13dB

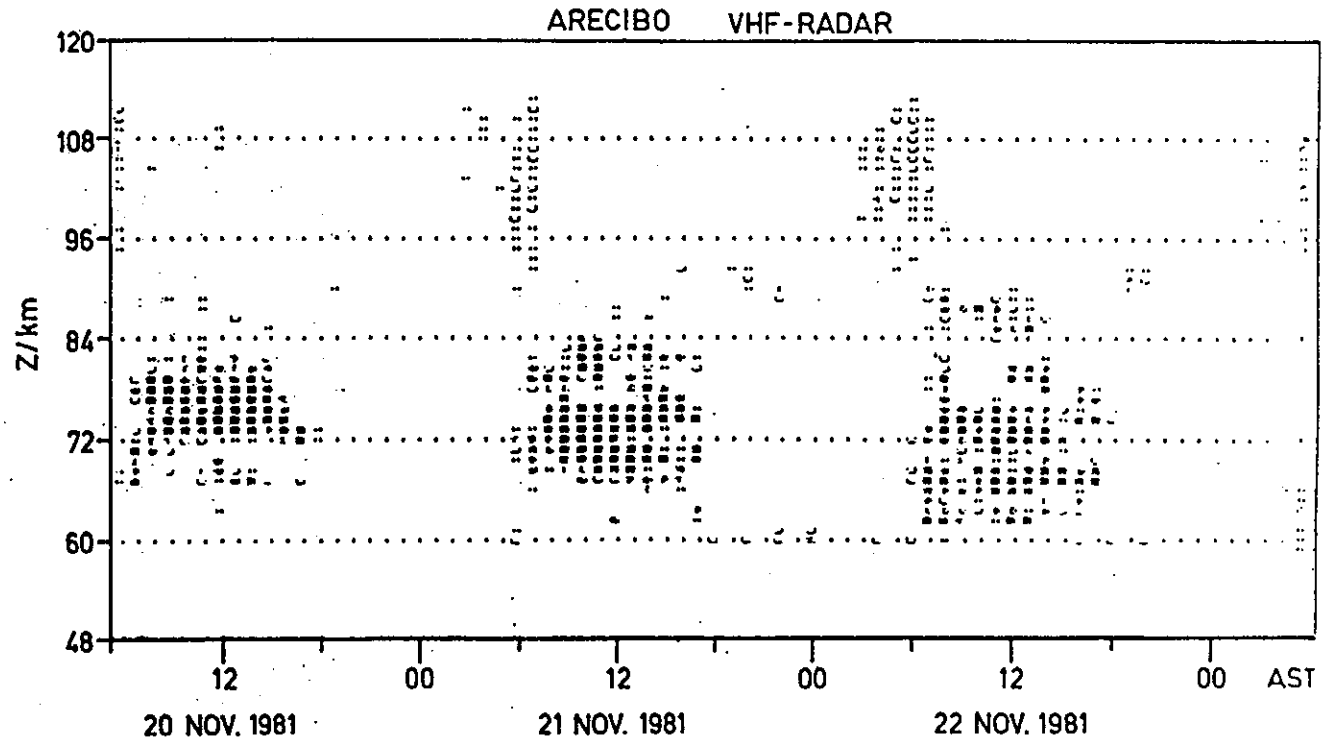
ARECIBO VHF-RADAR
120
108
96
84
72
60
48
Z/km
12
00
12
00
12
00
AST
20 NOV. 1981
21 NOV. 1981
22 NOV. 1981

A37

Mesosphere-Stratosphere-Troposphere Radar

These radars originate from the incoherent scatter radar in Jicamarca, Peru, which in the early 1980's detected non-incoherent scatter echoes from the mesosphere and also echoes from the stratosphere.

These radars are also known as VHF radars since they are operated in the low VHF band (around 50 MHz), which allows to detect echoes from the mesosphere in addition to those echoes from the stratosphere and troposphere. Echoes are observed from the cloudy as well as the clear air due to scattering from refractive index irregularities in electron density (mesosphere), neutral density and temperature (stratosphere) and neutral density, temperature and humidity (troposphere).

The observations with MST radars cover continuously the altitude range between about 1 - 15 km with a typical resolution of 150 - 1000 m in altitude and a few seconds to some minutes in time.

Typically, their power-aperture product is between 10^7 and 10^{10} Wm^2 (more than several 100 m^2 antenna area and more than several ten kW peak power) and their beam pointing direction is usually not exceeding 20 degrees zenith angle.

A3(

These radars apply the special modes of Doppler beam swing (DBS) and spaced antenna (SA), the latter frequently in the interferometer mode.

They are used to measure for instance:

Morphology of turbulence
e.g. intensity, intermittency, thickness and anisotropy

Stability
e.g. air mass mixing zones (fronts), inversion layers and tropopause

Velocity field:

mean horizontal and vertical velocities
i.e., prevailing winds and tides

fluctuating (oscillating) velocities
i.e. gravity waves and turbulence

spatial and temporal covariances
i.e. momentum flux

ST Radar Stratosphere-Troposphere Radar

These radars are simply the smaller version of MST radars and work at the same principle. Their power-aperture product is smaller (less than about 10^7 Wm^2 at VHF), which significantly limits their capability to detect weak mesospheric echoes. Most of these ST radars are operated at low VHF (50 MHz) but some also in the UHF band at 400-450 MHz. The latter are not at all capable to detect mesospheric echoes, however.

Wind Profilers

The ST radars, which are originally employed only as research instruments, have been developed into operational instruments, which are called Wind Profilers. Their principle is very comparable to that of the ST radars.

The Wind Profilers are operated in the low VHF band but more frequently in the UHF band around 400-450 MHz. They are designed to be operated unattendedly with a high time between failure and are manufactured commercially.

The data are analyzed on-line and the mean wind profiles are provided in real-time for meteorological applications in forecasting.

A-

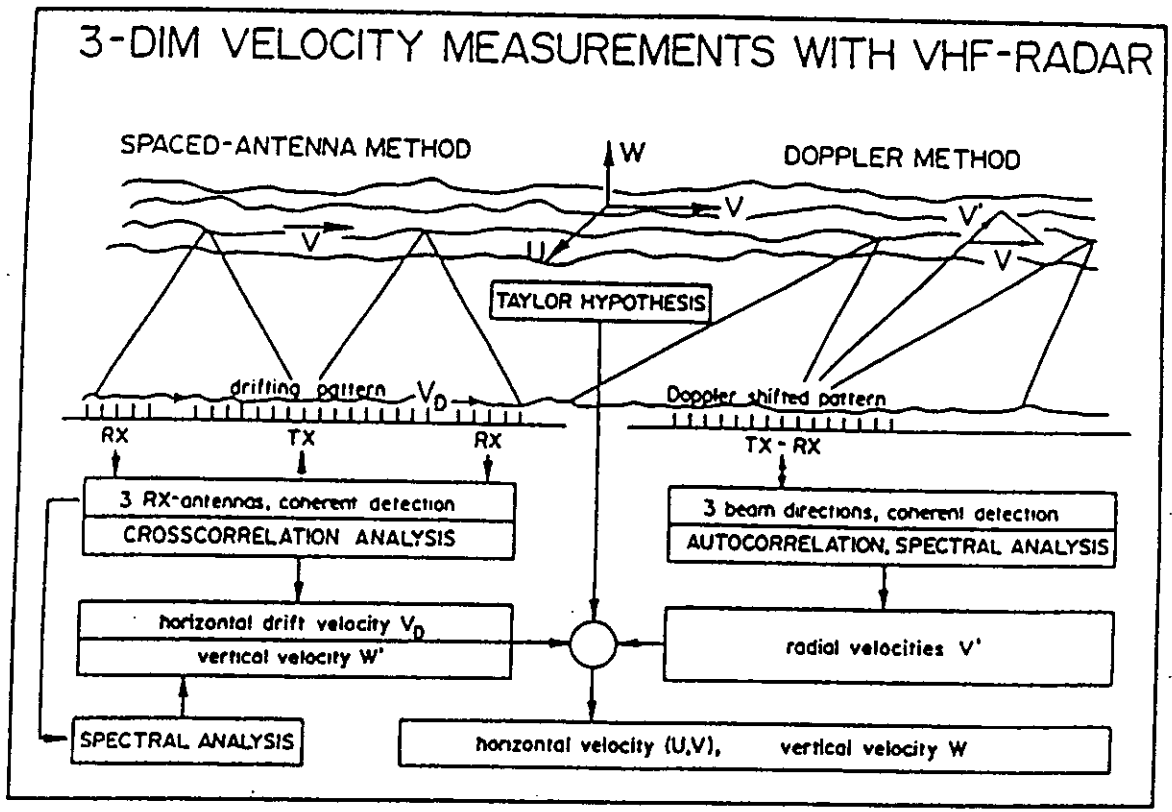
3-DIM VELOCITY MEASUREMENTS WITH VHF-RADAR
SPACED-ANTENNA METHOD
W
DOPPLER METHOD
V
V'
V'
V
U
TAYLOR HYPOTHESIS
drifting pattern V_D
Doppler shifted pattern
RX
TX
RX
TX - RX
3 RX-antennas, coherent detection
CROSSCORRELATION ANALYSIS
3 beam directions, coherent detection
AUTOCORRELATION, SPECTRAL ANALYSIS
horizontal drift velocity V_D
vertical velocity W'
radial velocities V'
SPECTRAL ANALYSIS
horizontal velocity (U,V), vertical velocity W

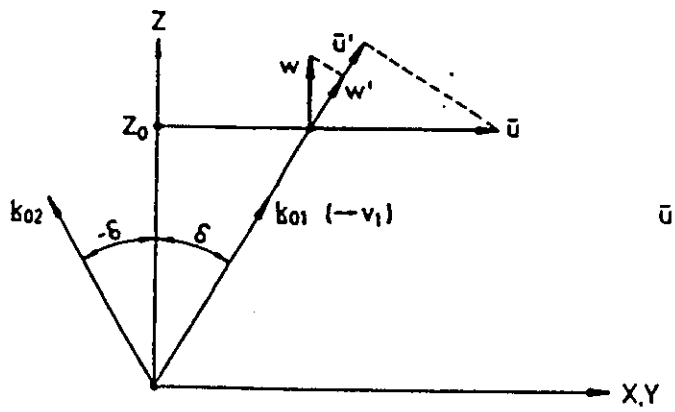

$$\bar{u} = \frac{v_1 - v_2}{2 \sin \delta} \quad , \quad w = \frac{v_1 + v_2}{2 \cos \delta}$$

Figure 9. Principle geometry of two antenna beam directions $\underline{k}_{o1}$ and $\underline{k}_{o2}$ at zenith angles δ and $-\delta$ for the deduction of the horizontal velocity component u and the vertical velocity component w. The measured radial velocity components v_1 and v_2 consist of the projections u' and w' of the u and w velocity components, respectively.

A

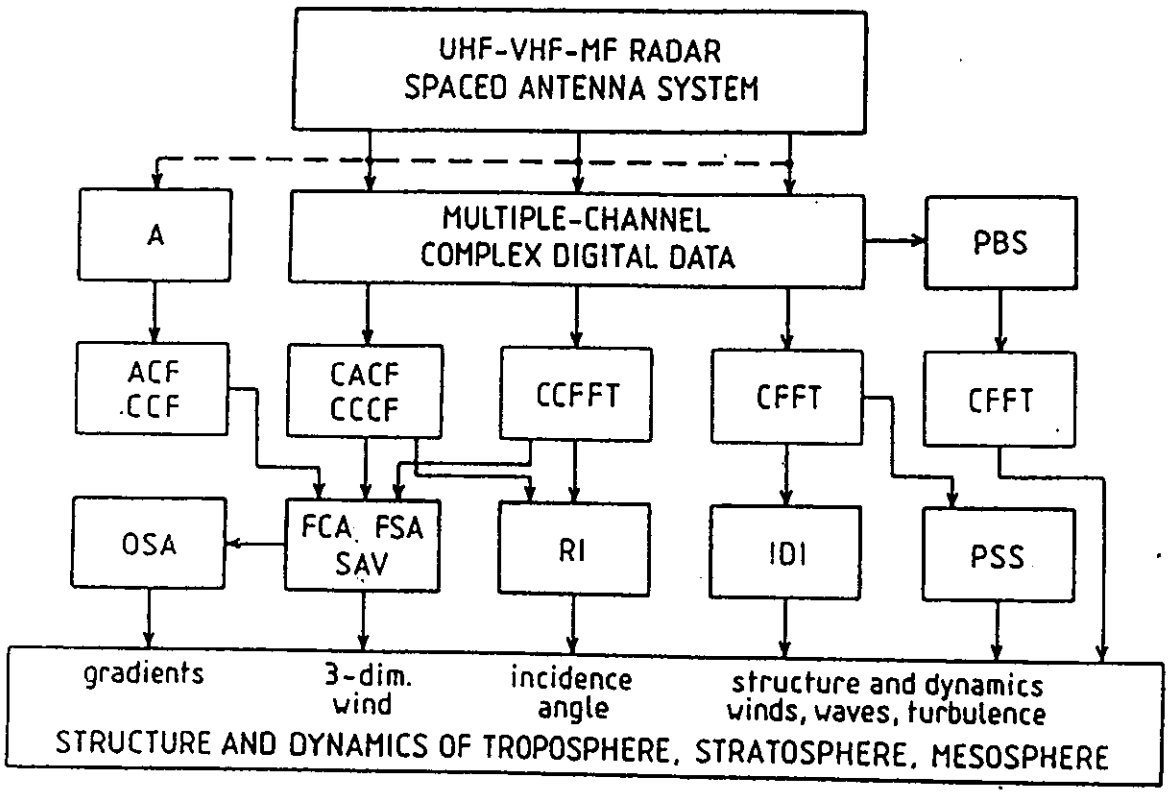

Fig. 1 Methods to analyze radar signals detected with spaced antenna arrays in UHF, VHF and MF radar systems to investigate the structure and dynamics of the lower and middle atmosphere.

Lightning radar studies

Essentially narrow beam X-, C-, S-, and UHF weather radars at wavelengths between 3 cm and 68 cm had been used to study scatter from lightning. It is assumed that the scatter results from the high electron density generated in the lightning channels. There is evidently quite some similarity with scatter from meteor trails, however, due to the dendritic structure of lightning channels and their very short lifetime, the scattering process is much more difficult to understand.

At these relatively short wavelengths (< 68 cm) used so far, the power of the scatter power from lightning is usually in the same order as that of the echo from the surrounding precipitation.

It was recently shown that lightning echoes can also be significantly studied with VHF ST radars. However, here the coherent integration time has to be substantially reduced, since a time resolution of a few milliseconds is needed to investigate the highly non-stationary lightning echo. By means of radar interferometry the three-dimensional lightning structure can be studied.

A 1

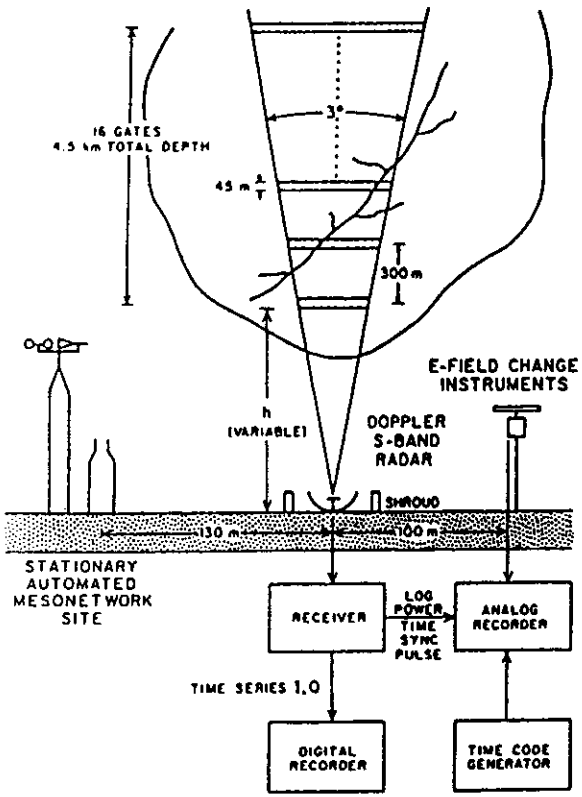

Fig. 1. Schematic of instrumentation and data recording used to observe lightning and storm structure overhead. The vertically pointing antenna has a 3° beamwidth within which data are recorded in range layers 45 m deep and spaced 300 m apart. The height h to the first layer can be varied, which moves the entire radar observational volume vertically.

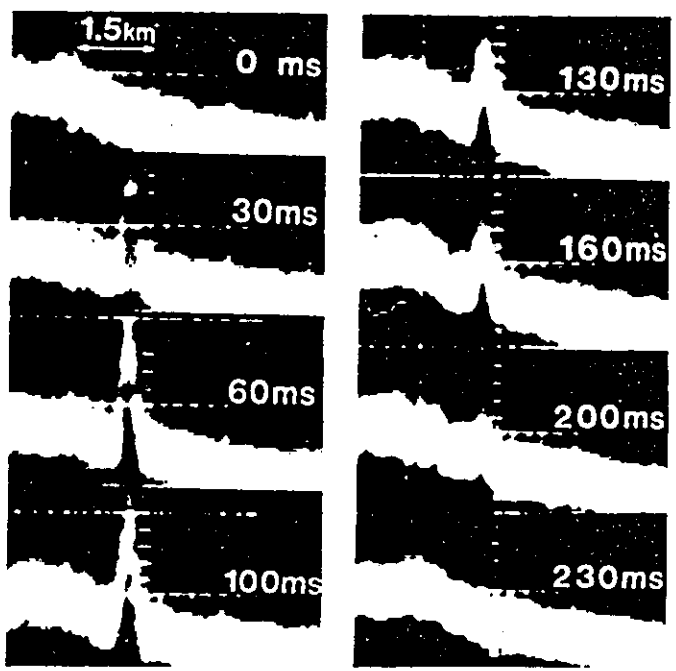

Fig. 3. Time evolution of a typical lightning echo obtained with the vertically pointing Doppler radar. This sequence was generated by photographing a TV display of the radar log video output. Time 0 is the frame immediately preceding the lightning flash, whose echo is clearly seen at t = 30 ms. The flash occurred on day 118 at about 0935:30 CST.

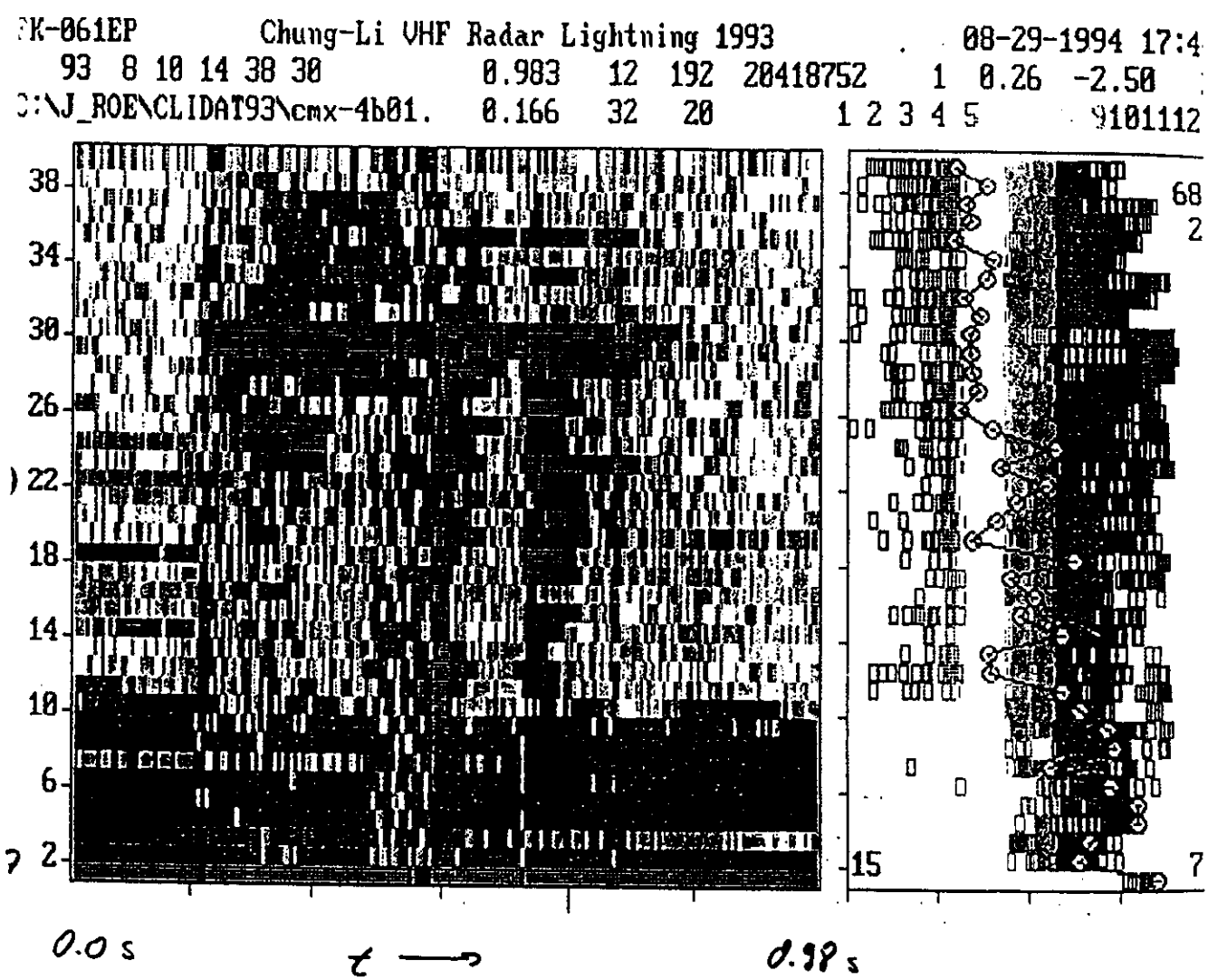
K-061EP Chung-Li VHF Radar Lightning 1993 08-29-1994 17:4
93 8 10 14 38 30 0.983 12 192 20418752 1 0.26 -2.50
:\J_ROE\CLIDAT93\cmx-4b01. 0.166 32 20 1 2 3 4 5 9101112
38
34
30
26
22
18
14
10
6
2
68
2
15
7
0.0 s
t
0.98 s

A4

Doppler Weather Radars

These radars are applied to investigate the tropospheric structure and dynamics by detecting scatter from precipitation (rain, hail and snow), occasionally also from the clear and cloudy air. The operating frequencies are above 1 GHz, since the scatter cross section of precipitation is inversely proportional to the fourth power of the wavelength. These radars are using parabolic dish antennas, which have to be pointed at all azimuth directions, usually at lower elevation angles. This research direction is mostly known as Radar Meteorology, which will not be treated in the context of this lecture (reference is made to the book "Radar in Meteorology", published by the American Meteorological Society).

ST radars for studies of precipitation

However, ST VHF and UHF radars are also detecting echoes from precipitation, which allows to determine for instance rain drop size distributions. The echoes from strong precipitation are about equal in amplitude to the usual ST radar echoes from the clear and cloudy air. It is essential that these echoes from precipitation can be separated from the common echoes in the Doppler spectra due to their fall velocity (measurable with the vertical beams of the ST radars), which is usually larger than the air velocity.

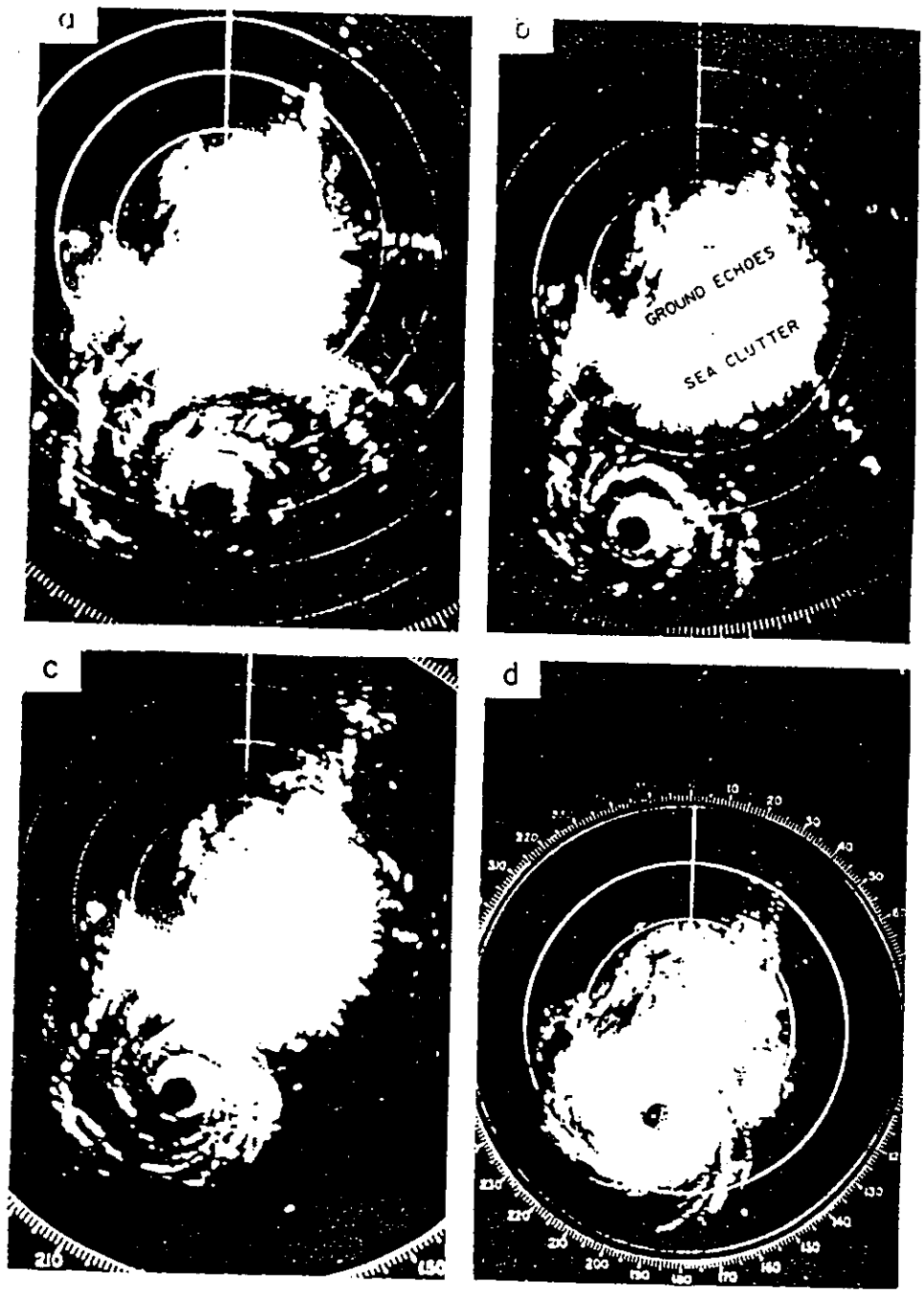

Fig. II.21. PPI pictures of typhoon Dacy taken with 10.4 cm MU Fan radar. Range markers are at 100 km intervals. a: 03 JST, 21 August 1965, elevation 1.5°. b: 10 JST, 21 August 1965, elevation 1.5°. c: 04 JST, 22 August 1965, elevation 1.5°. d: 11 JST, 22 August 1965, elevation 0.5°. From Tatehira and Fukuta (1966).

The reflectivities for clear air and precipitation can be estimated from the formulas

$$\eta_t = 0.38\lambda^{-1/3}C_n^{\,2}$$

$$\eta_p = \pi^5\lambda^{-4}|K|^2 Z$$

where η_t is the reflectivity for turbulent scatter and η_p is the reflectivity for scatter from precipitation

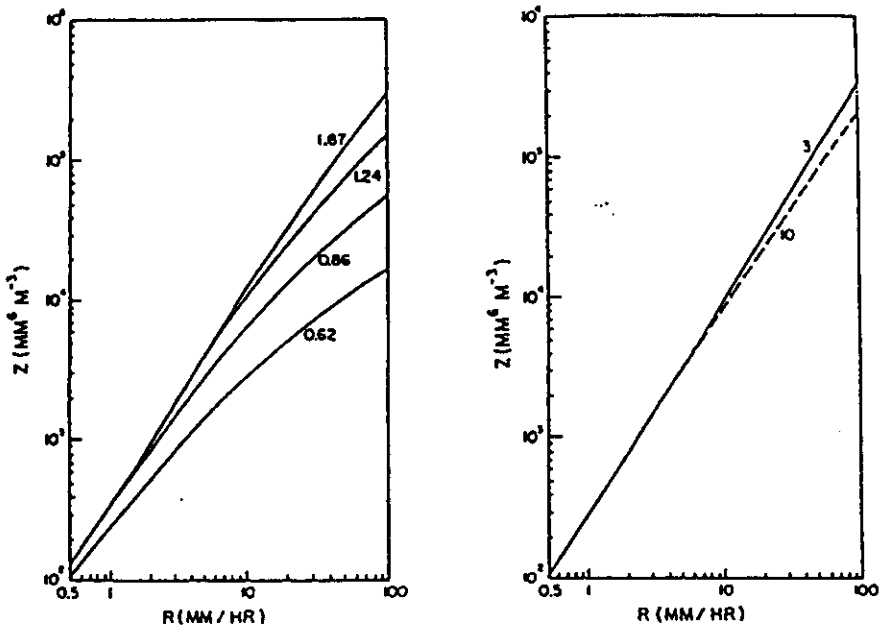

Plots of Z as a function of R computed using Mie scattering (solid lines) or Rayleigh scattering (dashed line) for MP drop-size distributions (from [Wexler and Atlas, 1963]).

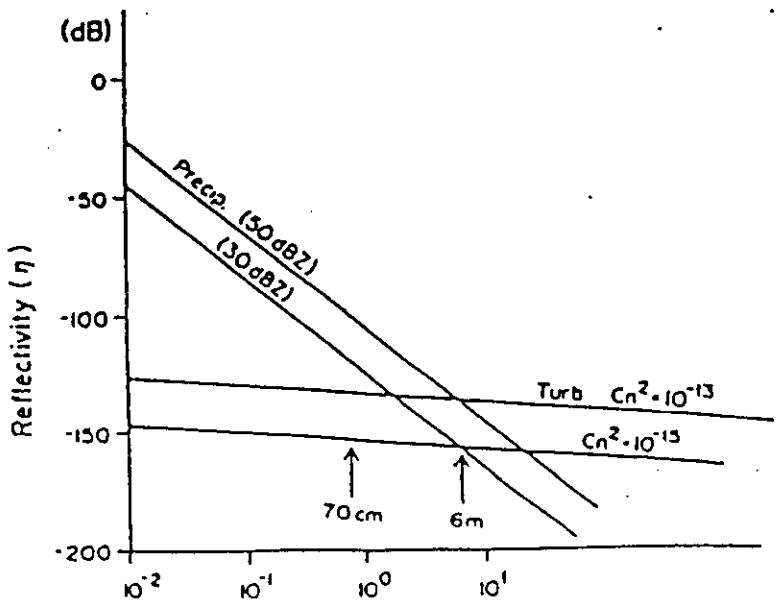

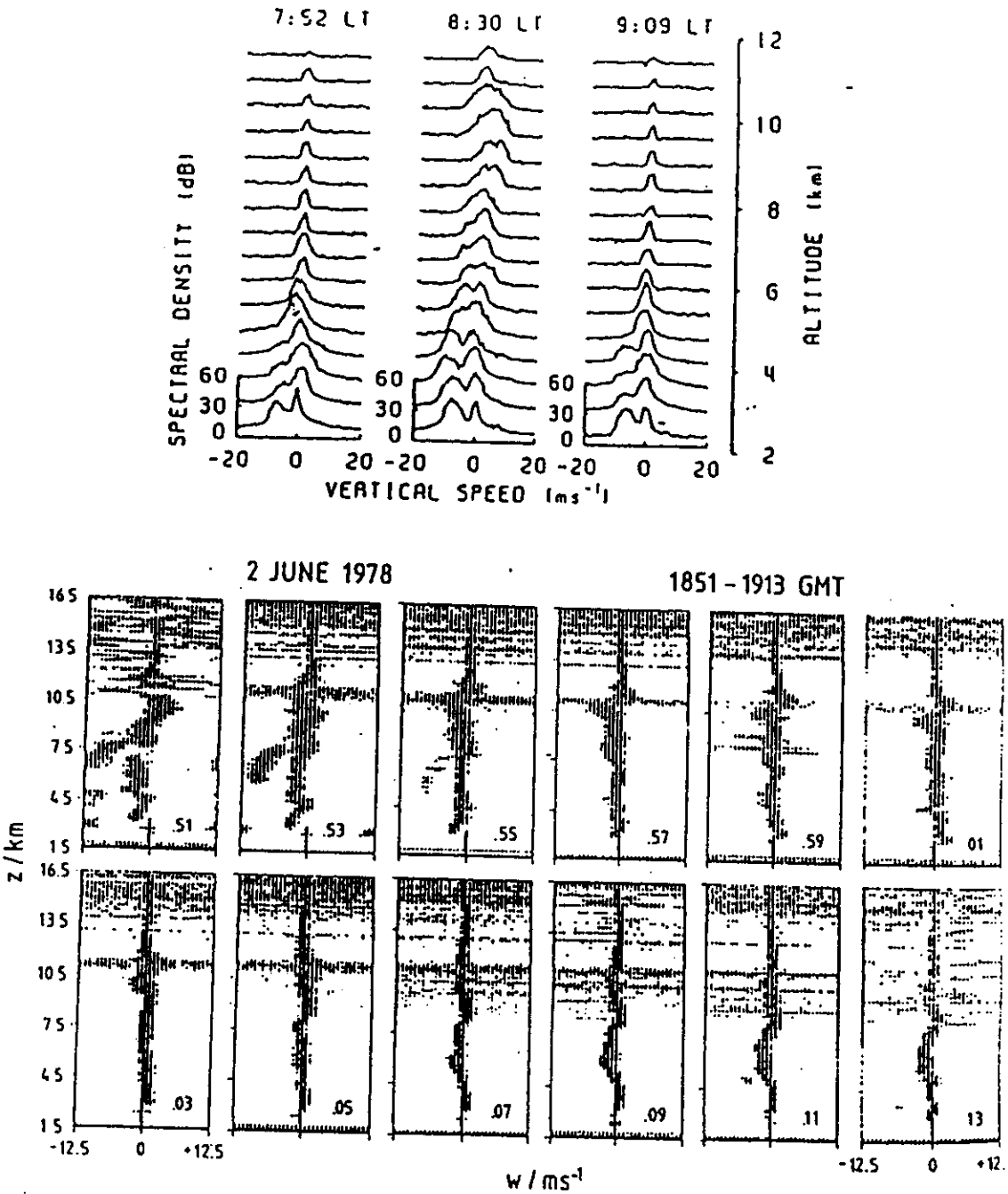

FIG. 3. Successive profiles showing reflected power as a function of Doppler shift (vertical velocity) and altitude during the overhead passage of a thundercloud for the SOUSY-VHF-Radar data. The time interval between profiles is 2 min. Note that the echoes with zero or positive upward velocities are due to scatter from turbulence while the echoes with large negative velocities at lower altitudes are due to scatter from precipitation.

A4

BLR **Boundary Layer Radar**

Boundary Layer Radars operate at higher frequencies than the ST radars, usually around 1 GHz. Their advantage is essentially instrumental, since lower altitudes can be sampled (< 100 m) and the range resolution is increased (< 30 m), and the antenna size is much smaller due to the higher frequency. Otherwise these BLRs are principally equivalent to the ST radars. The BLRs cannot reach as high as ST radars, essentially due to their smaller power-aperture product, but also due to smaller scatter cross section of the clear air, which decreases with wavelength and altitude. However, these BLRs are particularly designed and operated to study the planetary boundary layer, which has given them their name. They are also quite sensitive to precipitation due to their shorter operation wavelength.

FM-CW Radar

Frequency-Modulated Continuous Wave Radar

These kinds of radars are also used to study particularly the planetary boundary layer and allow a very high range resolution due the application of wide-bandwidth frequency-modulation. They are operated at frequencies of several GHz in a quasi-monostatic mode (due to the application of CW, the receiving and transmitting antennas have to be separated/decoupled).

CHRISTMAS ISLAND (Rep. of KIRIBATI)
Composite Zonal Wind Profile (50 MHz & 915 MHz Systems)
8 Nov. 1986 ($09^h\ 30^m$ — $14^h\ 30^m$ L.T.)

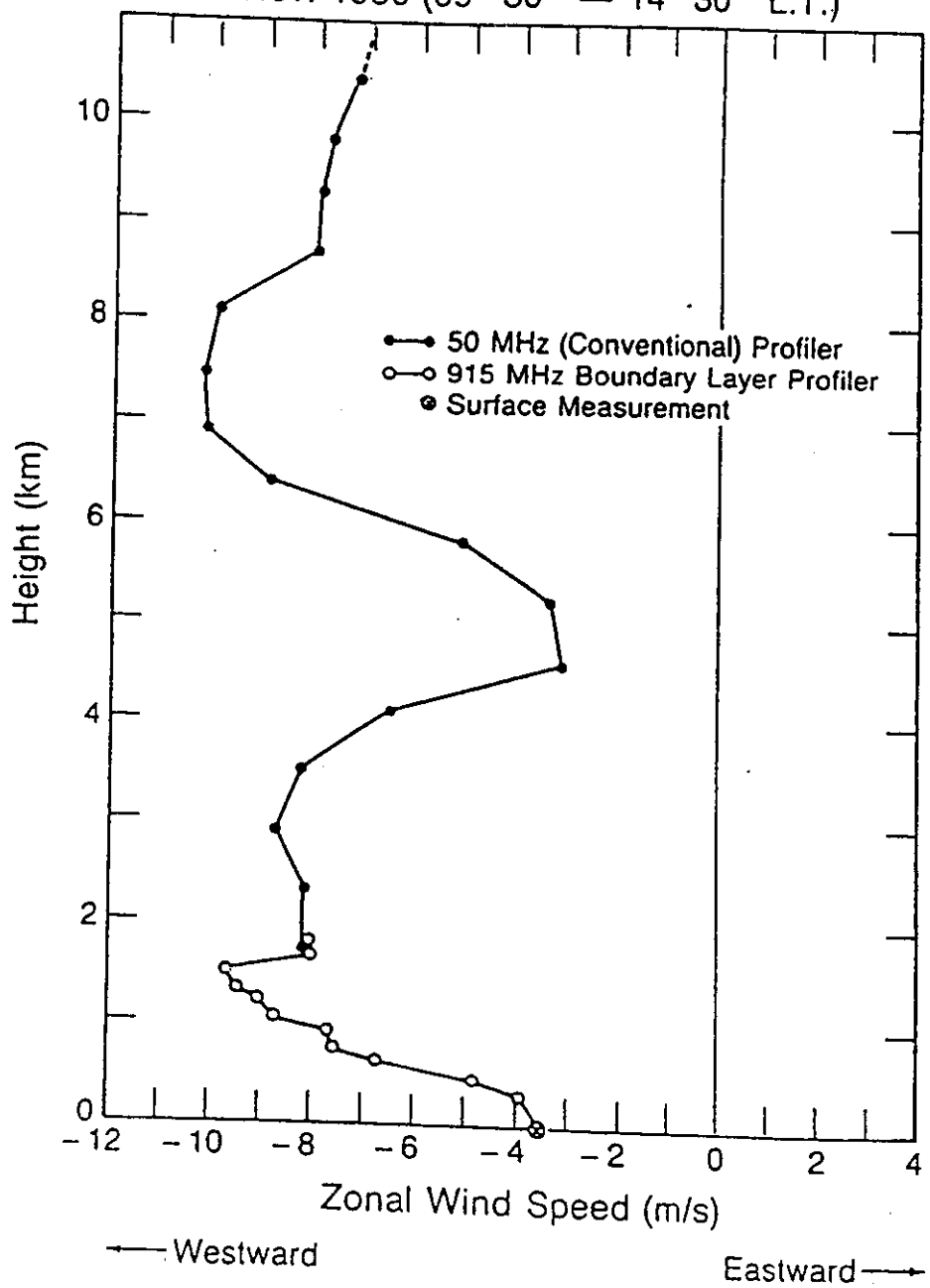

A5

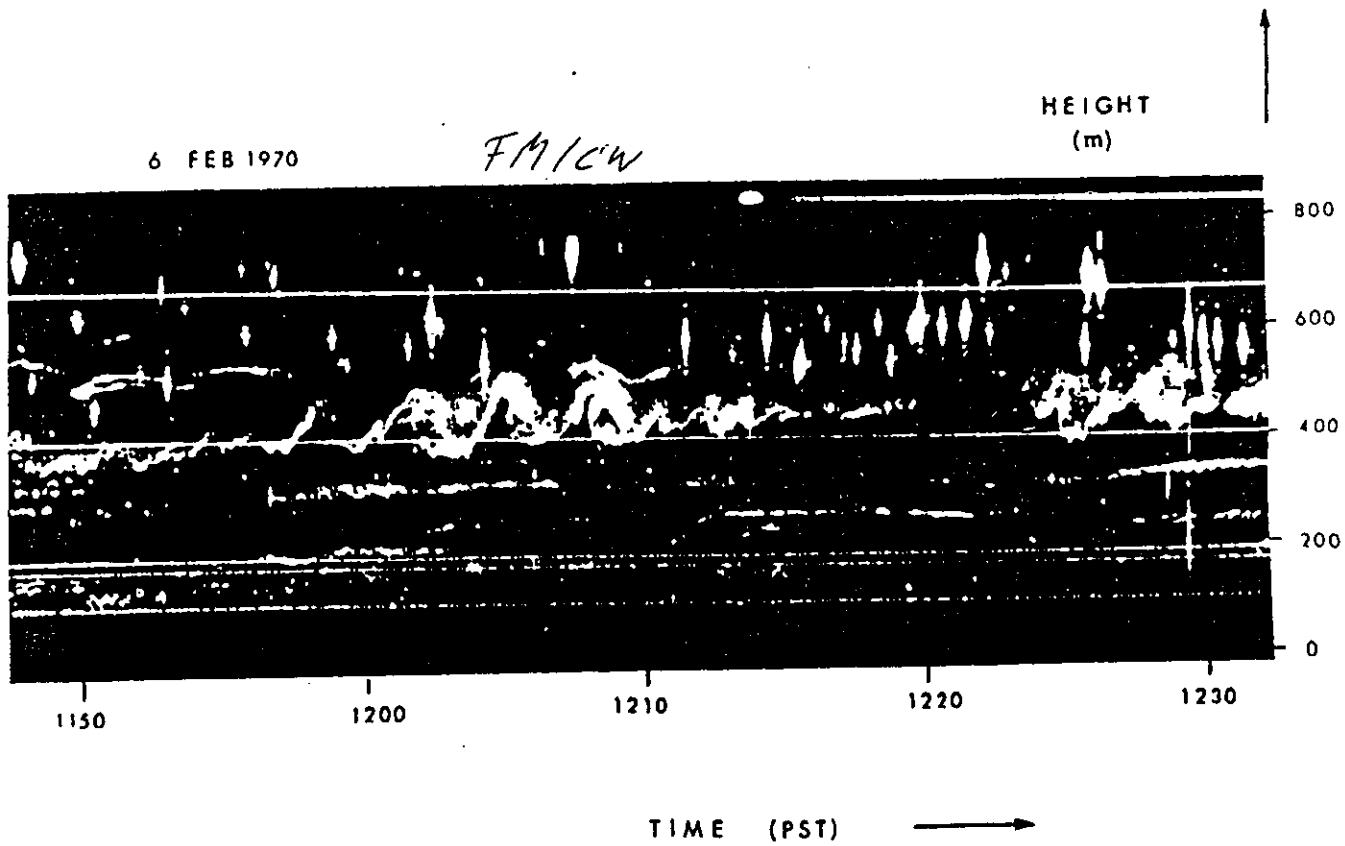
6 FEB 1970
FM/CW
HEIGHT
(m)
800
600
400
200
0
1150
1200
1210
1220
1230
TIME (PST)

Bi-static radar observations

In almost all cases of radar studies of the atmosphere, mono-static radars are used (i.e., the radar transmitter and receiver are at the same location). Bi-static radar observations are made by separating the radar receiver (antenna) from the radar transmitter (antenna). The advantage of such observations is that a CW signal can be transmitted, which increases the average power and in turn the sensitivity. It is essential to assure overlapping of the beams of the transmitting and the receiving antennas. With a single beam receiving antenna of limited beam width, only a small common volume can be measured at a time. With narrow antenna beams this allows a high spatial resolution, which can be increased further by long binary coding of the transmitted signal. Only S-band bi-static radar observations of stratospheric turbulence are known.

Dual Doppler radar

This technique seems to have some similarity to bi-static radar observations, since radars at separate locations are used. However, these are operated in mono-static mode, i.e measuring the radar reflectivity and the radial velocity along each single radar beam. This technique has not been used (and may not be very suitable) in MST radar applications, but only in Doppler weather radar observations, for instance to study severe storms.

A

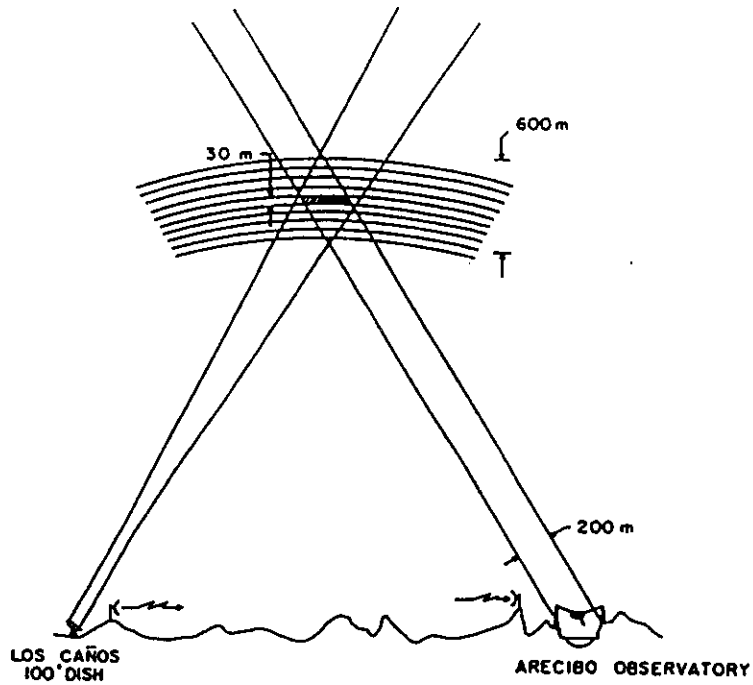
600 m
30 m
200 m
LOS CAÑOS
100' DISH
ARECIBO OBSERVATORY

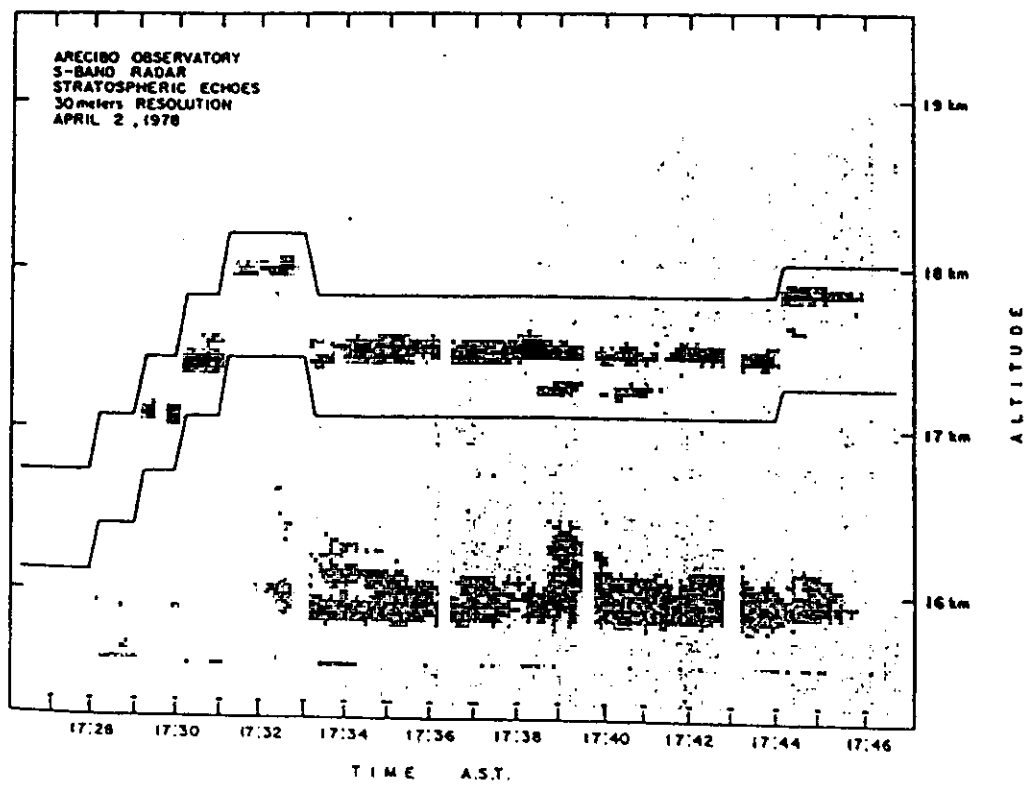
ARECIBO OBSERVATORY
S-BAND RADAR
STRATOSPHERIC ECHOES
30 meters RESOLUTION
APRIL 2, 1978
19 km
18 km
17 km
16 km
ALTITUDE
17:28
17:30
17:32
17:34
17:36
17:38
17:40
17:42
17:44
17:46
TIME A.S.T.

RASS Radio Acoustic Sounding System

Radar waves are scattered from refractive index variations at half the radar wavelength (Bragg condition for mono-static backscatter). These variations can be artificially created by means of acoustic (sound) waves. The acoustic waves propagate longitudinally with the velocity of sound. If the wave vectors of the radar wave and the acoustic wave match, the radar echo will be enhanced.

The Bragg pattern moves with the sound velocity and the background wind velocity. Due to this velocity the radar wave scattered back from the Bragg pattern undergoes a Doppler shift. By measuring this Doppler shift the velocity can be determined. Considering the wind velocity, measured independently with the standard ST radar technique, the sound velocity can be determined . Since the sound velocity depends on temperature, the latter can be measured with this method.

The basic requirement of matching wave vectors is difficult to obtain: The attenuation and variation of the propagation path of the acoustic wave often makes the measurement even more demanding. This technique has been successfully applied with VHF and UHF radars. A high power acoustic transmitter is needed (acoustic frequencies are in around 100 Hz) to be operated with the ST radar.

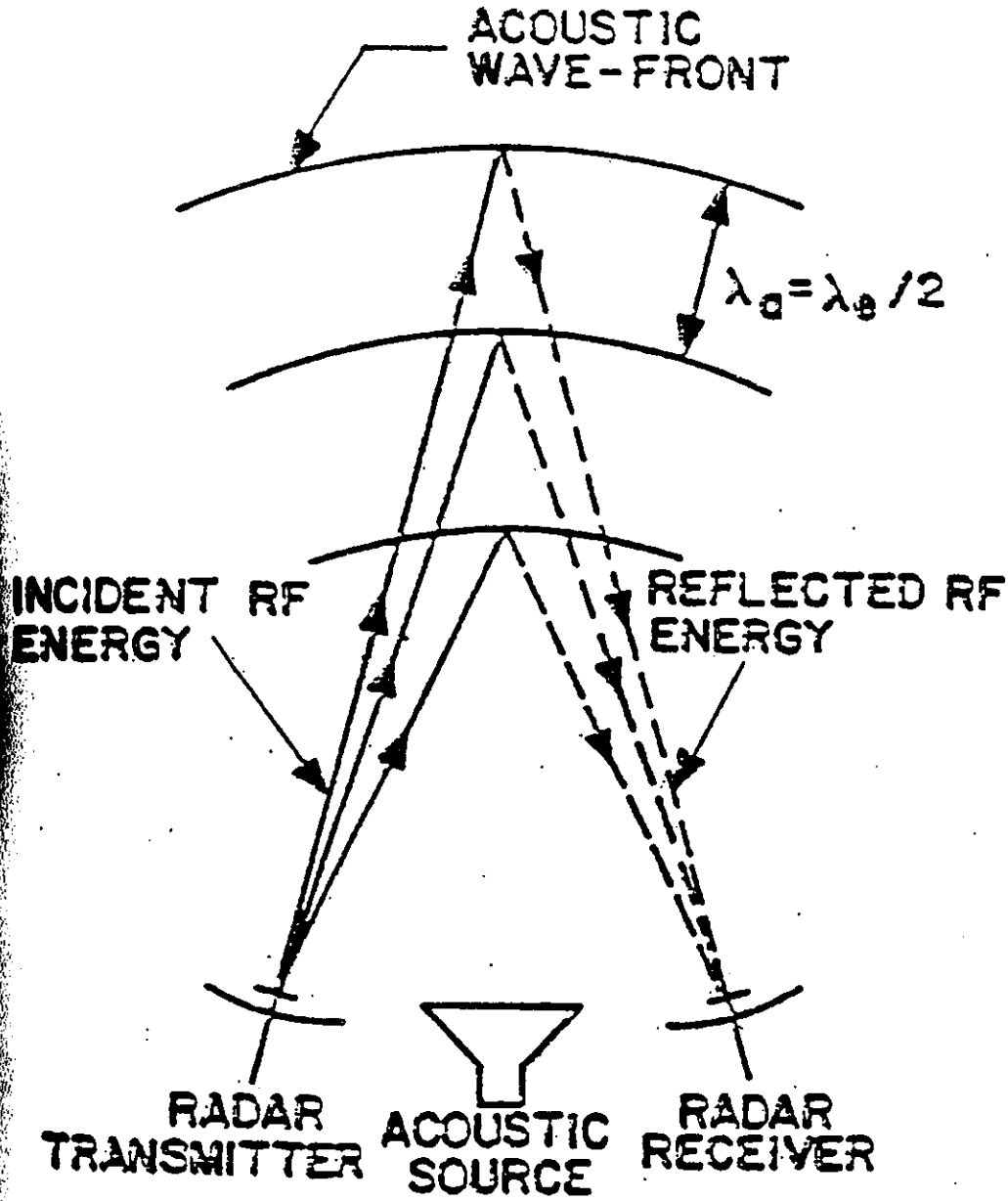

RASS BISTATIC GEOMETRY

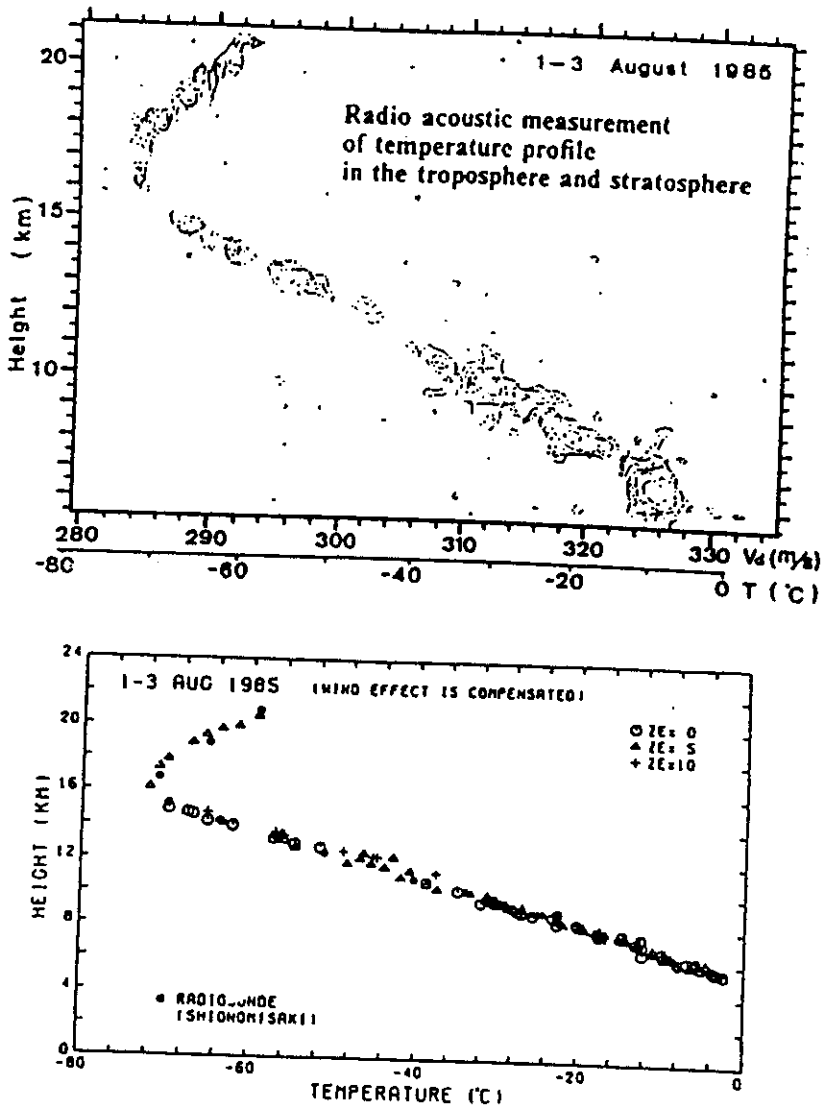

Fig. 9.2a Contours of RASS echo power caused by acoustic waves at frequencies between 88 and 101 Hz measured with 46.5-MHz MU radar between 1–3 August 1985.

Fig. 9.2b Temperature profile derived from the RASS echoes shown in Fig. 9.2a compared with a temperature profile obtained from radiosonde measurements (closed circles) (from Matuura et al., 1986; reprinted by permission from Nature, *Vol. 323, pp. 426–428, copyright ©1986, Macmillan Magazines Ltd.).*

API Artificial Periodic Inhomogeneities

HF radio waves transmitted vertically into the ionosphere are undergoing total reflection when they reach the level of critical frequency (radio wave frequency is equal to the plasma frequency). With the upward travelling wave the reflected wave forms a standing wave pattern. This periodic wave structure modulates the electron density (in the D-region by electron heating, which affects the electron attachment to the neutrals) and forms a Bragg screen, from which such HF waves matching the Bragg condition in the ionosphere (half the wavelength equals the spatial electron density variation scale) are backscattered. The scatter cross section is artificially enhanced by this process. The technique of API had been successfully tested in such a way that the standing wave pattern is built up over several seconds by a powerful transmitter (e.g. an ionospheric heating or modification facility). When the modification transmitter is turned off, the pattern still remains for a while and can be sensed by a sounding MF/HF radar wave. By measuring the amplitude decay time of API echoes from the D-region the electron attachment and detachment coefficients can be determined and the Doppler shift gives the vertical velocity. This technique should be applicable in conditions where incoherent and coherent scatter from the mesosphere would be too weak to be detectable. It could constitute a useful complement to incoherent scatter and MST radars.

Summary of measured parameters and derived information from the API technique

Height Region	Measured parameter	Derived Information
All heights	Virtual height vs frequency	Electron density
F region	Amplitude, phase vs time	Electron, ion temperature
E region	Phase vs time Amplitude vs time	Vertical wind velocity Ambipolar diffusion coefficient
D region	Phase vs time Amplitude vs time	Vertical wind velocity Coefficient of electron attachment and detachment

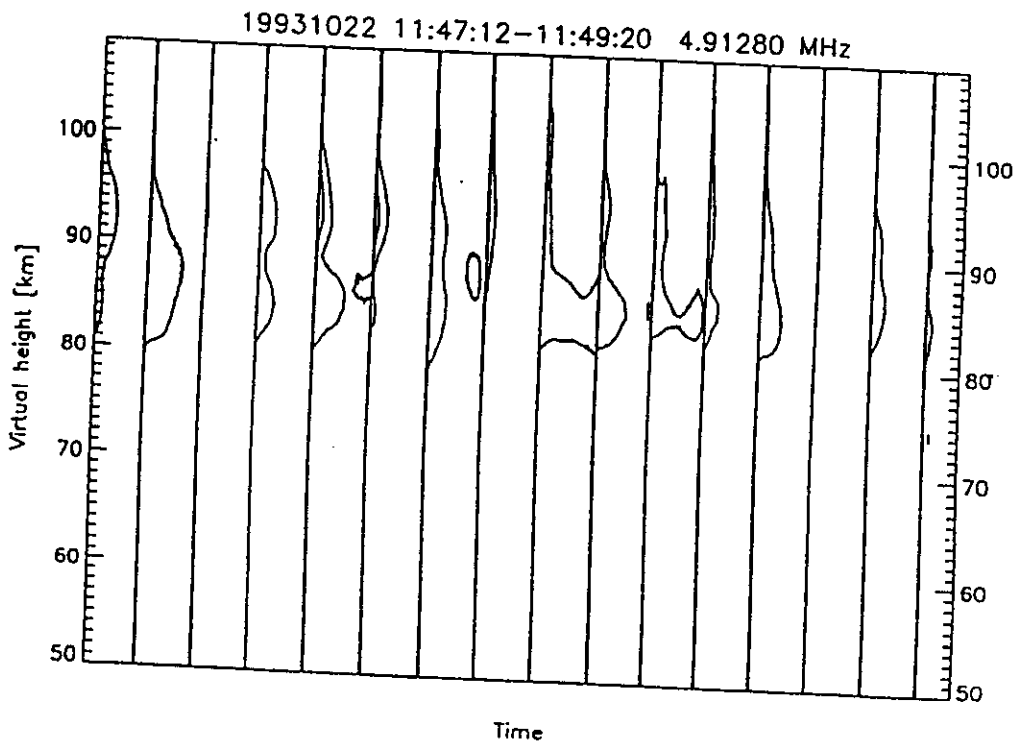

Fig. 2. Contour plot of backscattered power at 4.9128 MHz, showing the decay of API in the height range 80-100 km. The spacing between vertical lines is 5.1 s. Each vertical line marks the end of a 4 s heater-on pulse and the start of a 5.1 s interval of radar probing using 60 μs pulses and 100 Hz repetition period.

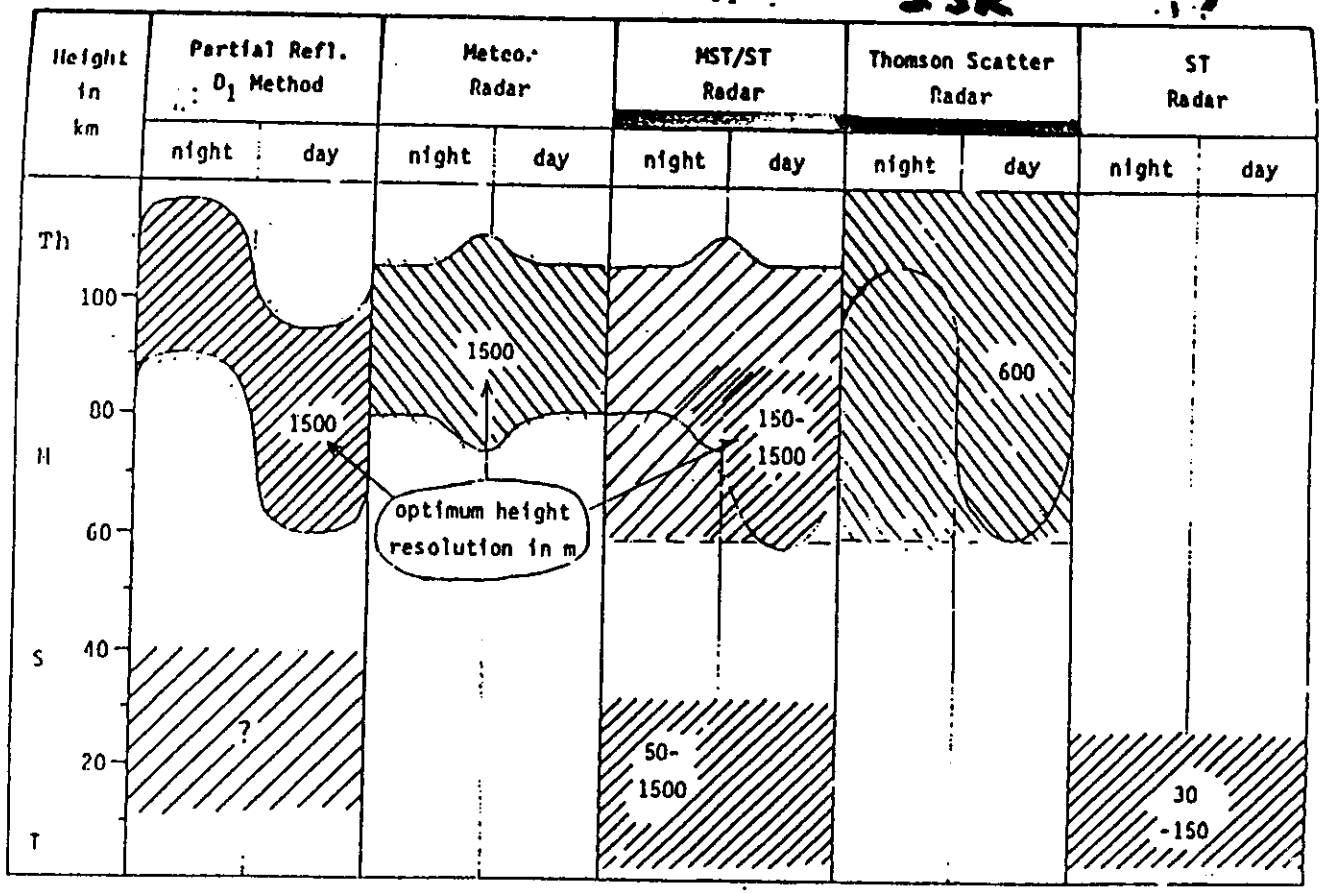
Height in km
Partial Refl. D_1 Method
Meteo. Radar
MST/ST Radar
Thomson Scatter Radar
ST Radar
night
day
night
day
night
day
night
day
night
day
Th
100
80
H
60
S
40
20
T
1500
1500
optimum height resolution in m
?
150-1500
600
50-1500
30-150

Radars provide a most suitable image of many atmospheric features of the lower, middle and upper atmosphere and they have become essential ground-based tools for unique atmospheric research and meteorological operations